arXiv:1101.1852v1 [hep-ex] 10 Jan 2011

# Hadron-Hadron and Cosmic-Ray Interactions at multi-TeV Energies

Mini-proceedings ECT* Workshop, Trento, Nov. 28 - Dec. 3, 2010

B. Alessandro[1], D. Bergman[2], M. Bongi[3], A. Bunyatyan[4], L. Cazon[5], D. d'Enterria [6,7], I. de Mitri[8,9], P. Doll[10], R. Engel[11], K. Eggert[7,12], M. Garzelli[13,14], L. Gerhardt[15], S. Gieseke[16], R. Godbole[7], J.F. Grosse-Oetringhaus[7], G. Gustafson[17], T. Hebbeker[18], L. Kheyn[19], J. Kiryluk[15], P. Lipari[20], S. Ostapchenko[21], T. Pierog[11], O. Piskounova[22], J. Ranft[23], A. Rezaeian[24], A. Rostovtsev[25], N. Sakurai[26], S. Sapeta[27], S. Schleich[28], H. Schulz[29], T. Sjöstrand[17], L. Sonnenschein[18], M. Sutton[30], R. Ulrich[31], K. Werner[32], and K. Zapp[33]

[1] *INFN Sezione di Torino, Torino, Italy*
[2] *University of Utah, Dept. Phys. & Astron., Salt Lake City, UT 84112, USA*
[3] *INFN Sezione di Firenze, Via Sansone 1, I-50019 Sesto Fiorentino, Firenze, Italy*
[4] *DESY, Notkestrasse 85, 22607 Hamburg, Germany*
[5] *LIP, Av. Elias Garcia 14 - 1o, 1000-149 Lisbon, Portugal*
[6] *ICREA & ICC-UB, Universitat de Barcelona, 08028 Barcelona, Catalonia*
[7] *CERN, PH Department, CH-1211 Geneva 23, Switzerland*
[8] *Dipartimento di Fisica, Università del Salento, I-73100, Lecce, Italy*
[9] *INFN Sezione di Lecce, I-73100, Lecce, Italy*
[10] *Institut für Experimentelle Kernphysik, KIT Campus Sued, 76021 Karlsruhe, Germany*
[11] *Karlsruhe Institute of Technology, P.O. Box 3640, 76021 Karlsruhe, Germany*
[12] *Case Western Reserve University, Cleveland, USA*
[13] *INFN Sezione di Milano, Milano, Italy*
[14] *Depto. Física Teórica y del Cosmos y CAFPE, Univ. de Granada, 18071 Granada, Spain*
[15] *Lawrence Berkeley National Laboratory, 1 Cyclotron Road, 94720 Berkeley, USA*
[16] *Institute for Theoretical Physics, Karlsruhe Institute of Technology, 76128 Karlsruhe, Germany*
[17] *Dept. of Astronomy and Theoretical Physics, Lund University, SE-223 62 Lund, Sweden*
[18] *RWTH Aachen University, Phys. Inst. IIIA, 52056 Aachen, Germany*
[19] *D.V. Skobeltsyn Institute of Nuclear Physics, Moscow State University, 119992 Moscow, Russia*
[20] *INFN Sezione di Roma, Roma, Italy*
[21] *NTNU, Institutt for Fysikk, 7491 Trondheim, Norway*
[22] *P.N.Lebedev Physical Institute of Russian Academy of Science, Moscow, Russia*
[23] *Siegen University, Siegen, Germany*
[24] *Depto. Física, Univ. Técnica Federico Sta. Ma., Casilla 110-V, Valparaiso, Chile*
[25] *Institute for Theor. & Exp. Physics, B.Cheremushkinskaya 25, 117218 Moscow, Russia*
[26] *Faculty of Science, Osaka City Univ., 3-3-138 Sugimoto, Sumiyoshi-ku, Osaka 558-8585, Japan*
[27] *LPTHE, UPMC Univ. Paris 6 and CNRS UMR 7589, Paris, France*
[28] *TU Dortmund, Univ. Dortmund, Exp. Physik 5, Otto-Hahn-Strasse 4, Dortmund, Germany*
[29] *Humboldt University, Inst. f. Physik, Newtonstr. 15, 12489 Berlin, Germany*
[30] *Dept. of Physics and Astronomy, University of Sheffield, S3 7RH Sheffield, UK*
[31] *Dept. of Physics, 104 Davey Lab, Penn State University, 16802 University Park, USA*
[32] *SUBATECH, 4 rue Alfred Kastler, BP 20722, 44307 Nantes Cedex 3, France*
[33] *IPPP, Science Laboratories, Durham Univ., DH1 3LE Durham, UK*

## ABSTRACT

The workshop on "Hadron-Hadron and Cosmic-Ray Interactions at multi-TeV Energies" held at the ECT* centre (Trento) in Nov.-Dec. 2010 gathered together both theorists and experimentalists to discuss issues of the physics of high-energy hadronic interactions of common interest for the particle, nuclear and cosmic-ray communities. QCD results from collider experiments – mostly from

the LHC but also from the Tevatron, RHIC and HERA – were discussed and compared to various hadronic Monte Carlo generators, aiming at an improvement of our theoretical understanding of soft, semi-hard and hard parton dynamics. The latest cosmic-ray results from various ground-based observatories were also presented with an emphasis on the phenomenological modeling of the first hadronic interactions of the extended air-showers generated in the Earth atmosphere. These mini-proceedings consist of an introduction and short summaries of the talks presented at the meeting.

## Contents


**1 Hadronic collisions at multi-TeV energies: Experiments** **5**

**2 Hadronic collisions at multi-TeV energies: Theory** **14**

**3 Cosmic-rays at Ultra-High Energies: Experiments** **23**

**4 Cosmic-rays at Ultra-High Energies: Theory** **28**

**A List of participants** **37**

**B Programme** **37**


## Introduction

The origin and nature of cosmic rays (CRs) with energies between $10^{15}$ eV and the so-called Greisen-Zatsepin-Kuzmin (GZK) cut-off at about $10^{20}$ eV [1], recently measured by the HiRes [2] and Auger [3] experiments, remains a central open question in high-energy astrophysics with very interesting connections to particle physics and, in particular, to Quantum-Chromo-Dynamics (QCD) at the highest energies ever studied. One key to solving this question is the determination of the elemental composition of cosmic rays in this energy range. The candidate particles, ranging from protons to nuclei as massive as iron, generate "extensive air-showers" (EAS) in interactions with air nuclei when entering the Earth's atmosphere. The determination of the primary energy and mass relies on hadronic Monte Carlo (MC) models which describe the interactions of the primary cosmic-ray in the upper atmosphere.

The bulk of particle production in such high-energy hadronic collisions can still not be calculated within first-principles QCD and general principles such as unitarity and analyticity (as implemented in Regge-Gribov theory) are often combined with perturbative QCD predictions for high-$p_T$ processes, constrained by the existing collider data ($E_{lab} \lesssim 10^{15}$ eV). Important theoretical issues at these energies are the understanding of diffractive and elastic hadronic scattering contributions, the description of hadronic forward fragmentation and multi-parton interactions ("underlying event"), and the effect of high parton densities ("gluon saturation") at small values of parton fractional momentum $x = p_{parton}/p_{proton}$. Indeed, at these energies, the relevant Bjorken-$x$ values are as low as $10^{-7}$, where effects like gluon saturation and multi-parton interactions, particularly enhanced with nuclear targets, are expected to dominate the early hadron collision dynamics.

The current energy frontier for hadron collisions in the laboratory is reached at the Large Hadron Collider (LHC), currently under operation at CERN. The measurement of inclusive hadron produc-

tion observables in proton-proton, proton-nucleus, and nucleus-nucleus collisions, at LHC energies (equivalent to $E_{lab} \approx 10^{17}$ eV) will provide very valuable information on high-energy multiparticle production, and allow for more reliable determinations of the CR energy and composition around the GZK cutoff. In the high luminosity phase of LHC, each bunch crossing will lead to several proton-proton interactions, increasing even more the importance of understanding the background from diffractive and soft particle production. Semi-hard particle physics will allow one to test the boundaries of the applicability of perturbative QCD in the region where low-$x$ gluon saturation phenomena become increasingly important and may even dominate particle production.

All LHC experiments feature detection capabilities with a wide phase-space coverage without parallel, in particular in the forward direction, compared to previous colliders [4]. Such capabilities allow for a (fast) measurement of global hadron-hadron collision properties (inelastic – including diffractive – cross sections, particle multiplicity and energy flows as a function of $p_T$ and pseudorapidity, ...) even with the moderate statistics of a first $pp$ and $PbPb$ run.

The aim of the Workshop was to discuss theoretical and experimental issues connected to hadronic interactions of common interest for high-energy particle and cosmic-ray physics. With the recent high-quality cosmic-ray results from the HiRes and Auger experiments and the first available LHC data it seemed a timely moment to have such a meeting in autumn 2010. The Workshop brought together experts, both theorists and experimentalists, in QCD and cosmic-ray physics in view of expanding the mutually beneficial interface between two communities currently exploring the physics of strong interactions at the highest energies accessible. The talks and discussions on various topics:

- QCD predictions for high-energy multiparticle production and their implementation in hadronic Monte Carlo generators: PYTHIA, HERWIG, SHERPA, PHOJET, DPMJET, QGSJET, SIBYLL, EPOS, QGSM, FLUKA;
- theoretical and experimental developments on diffractive and elastic scattering at high energies;
- theoretical approaches of multi-parton dynamics and underlying event in hadronic collisions;
- theoretical and experimental developments on low-$x$ QCD and inclusive particle production;
- theoretical developments on modeling of cosmic-ray showers;
- latest experimental QCD results at colliders: LHC (ATLAS, CMS, ALICE, LHCb, TOTEM, LHCf), Tevatron, RHIC, and HERA;
- latest cosmic-rays measurements in the $10^{15}$-$10^{20}$ eV range: Auger, HiRes, TA, Kascade-Grande, Argo, IceCube;

were organized around four main blocks:

1. Hadronic collisions at multi-TeV energies: Experimental results
2. Hadronic collisions at multi-TeV energies: Theory
3. Cosmic-rays at Ultra-High Energies: Experimental results
4. Cosmic-rays at Ultra-High Energies: Theory

These mini-proceedings include a short summary of each talk including relevant references, the list of participants and the workshop programme. We felt that such a format was more appropriate than full-fledged proceedings. Most results are or will soon be published and available on arXiv. Most of the talks can also be downloaded from the workshop website:

`http://www.cern.ch/CRLHC10/`

We thank the ECT* management and secretariat, in particular Cristina Costa, for the helpful cooperation prior and during the workshop and all participants for their valuable contributions. We believe that this was only the first workshop of this kind and look forward to similar meetings in the future.

DAVID D'ENTERRIA, RALPH ENGEL, TORBJÖRN SJÖSTRAND

# 1 Hadronic collisions at multi-TeV energies: Experiments

### First QCD results from the ATLAS Collaboration

*Mark Sutton*[1] *(University of Sheffield)*

Since the first LHC operation in Nov. 2009 the ATLAS experiment has collected data at several proton-proton centre-of-mass energies with an integrated luminosity of 45 pb$^{-1}$ in collisions at 7 TeV. This large sample has enabled many QCD-related analyses to be performed spanning the entire kinematic range from soft QCD in minimum bias interactions [5, 6] through to the study of the underlying event [7] in events with at least one energetic track, through to production of jets with high transverse momentum $p_T$ [8, 9]. Events with a prompt photon or a $Z$ or $W$ have also been observed copiously [10, 11] as have events where the gauge boson is produced in conjunction with a high-$p_T$ jet [12].

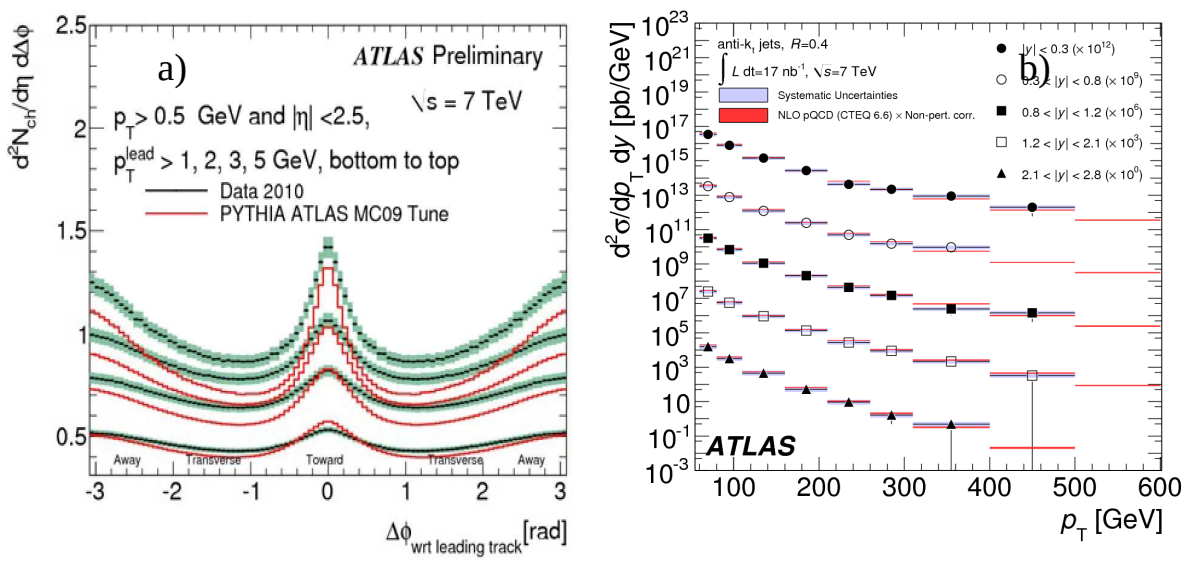


Figure 1: a) The particle azimuthal separation with respect to the leading particle in MB interactions. b) The inclusive single jet cross section, doubly differential in the jet $p_T$ and rapidity.

The charged particle multiplicity data from the analysis of minimum bias (MB) events [5–7] have already, and will continue to prove invaluable for the study of soft QCD and the underlying event (UE). Figure 1a shows the azimuthal separation between the particles and the leading particle for MB events for different requirements on the leading particle $p_T$. The increased collimation of the event with increasing leading particle $p_T$ illustrating the onset of hard QCD can be clearly seen. For the Monte Carlo tune shown, the particle multiplicity transverse to the leading particle is too low and the MC events themselves appear more collimated than the data. Figure 1b shows the inclusive single jet cross section doubly differential in the jet $p_T$ and rapidity. Within the large uncertainties, the NLO prediction corrected for hadronisation and UE describes the data well over five orders of magnitude.

The LHC has been working well and after less than a year of collisions at 7 TeV is already providing a large range of valuable physics data. Despite the large range of high quality results

[1] On behalf of the ATLAS collaboration.

already available from the ATLAS Collaboration, these only begin to explore the available phase space. Many analyses are still statistically limited in the most interesting regions of phase space and the Collaboration is working hard to reduce the systematic uncertainties. Given the status of the statistical and systematic uncertainties, perturbative QCD appears to be in reasonable shape.

**First CMS results**

*Thomas Hebbeker*[2] *(RWTH, Aachen)*

In the year 2009 the LHC collider at CERN started with proton proton collisions at a center of mass energy of 900 GeV, later the energy was increased to 2.36 TeV and in March 2010 a 7 TeV run began which ended in November 2010. The CMS experiment [13] has recorded about 40/pb of integrated luminosity at this record energy. The CMS detector performed very well and many interesting measurements were made. Lead-lead collisions at a total center of mass energy of 574 TeV at the end of 2010 brought new insights into heavy ion physics. First of all the CMS collaboration has 're-discovered' all Standard Model particles, including W and Z bosons decaying leptonically, the heaviest quark top and the lighter quarks in form of various meson and baryon resonances. These analyses demonstrate that the detector has reached the design values for efficiency and resolution. The inclusive jet [14] and dijet [15] production cross sections were among the first CMS measurements. The figure [14] shows that QCD calculations can reproduce the jet yields very well.

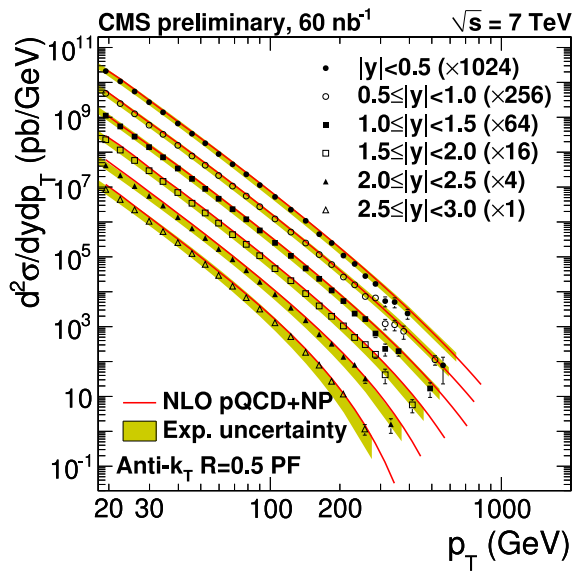


Figure 2: Jet spectra measured at various rapidities in $pp$ at 7 TeV compared to NLO pQCD.

The production of charged particles in minimum bias events (more precisely: in Non Single Diffractive events) was studied in great detail, in the pseudorapidity range $|\eta| < 2.4$ and for transverse momenta as low as 30 MeV/c. In particular the yield as a function of $\eta$, the multiplicity distribution and the $p_T$ distribution were determined at 0.9 TeV, 2.36 TeV and 7 TeV and compared to different model predictions and to data at other center of mass energies [16]. Furthermore the production of strange particles like the $\Xi^-$ were measured [17]. Overall the increase of cross sections and multiplicity with center of mass energy is steeper than anticipated. The current models with parameters tuned without using LHC data do not provide a satisfactory description in all details. Also the shape of jets

[2]On behalf of the CMS collaboration.

and the topology of hadronic events in general were analysed in detail [18, 19]. The models PYTHIA and HERWIG provide a good description of these CMS measurements. A very interesting new feature was discovered in $pp$ events with a very high charged particle multiplicity ($N_{ch} > 110$, $p_T = 1-3$ GeV/c). In the two-particle correlation as a function of $\Delta\eta$ and $\Delta\phi$ a 'ridge' structure, a long range correlation in $\Delta\eta$ at small values of the azimuthal distance $\Delta\phi$ was revealed by CMS [20]. Current Monte Carlo models cannot explain this feature. Finally already after a few days the first interesting heavy ion results were made public by CMS [21]: Z boson production in lead-lead collisions and 'jet quenching', seen as dijet events with very different energies carried by the two jets.

Beyond QCD results, from the smooth falloff of the measured dijet cross section as a function of dijet mass one can set limits on new particles. For example excited quarks can be excluded within a contact interaction model up to a mass of 1.58 TeV at 95% confidence level [15], thus improving older Tevatron limits significantly. From more than 100'000 W decays and about 10'000 Z decays their production cross sections were measured, these results are in good agreement with NNLO QCD calculations [22]. Also a first measurement of the top cross section was made [23], confirming the expected strong rise (by a factor of about 25) with respect to proton - antiproton collisions at 2 TeV center of mass energy.

**Charged-particle multiplicity in $pp$ and heavy-ion collisions at collider energies**

*Jan Fiete Grosse-Oetringhaus (CERN)*

The topical review [24] summarizes and critically reviews measurements of charged-particle multiplicity distributions and pseudorapidity densities in pp($\bar{p}$) collisions between $\sqrt{s}$ = 23.6 GeV and 1.8 TeV. Related theoretical concepts are briefly introduced: Feynman scaling which is based on phenomenological arguments about the exchange of quantum numbers predicts that the average number of charged particles increases with $\log\sqrt{s}$ which implies that the rapidity density $dN_{\rm ch}/dy$ is a constant as function of $\sqrt{s}$. Feynman scaling is not fulfilled in the measured energy range. KNO scaling postulated by Koba, Nielsen and Olesen in 1972 asserts that the multiplicity distribution falls onto a universal curve when rewritten as $P(N_{\rm ch}) \to 1/\langle N_{\rm ch}\rangle P(z)$ with $z = N_{\rm ch}/\langle N_{\rm ch}\rangle$. KNO scaling is valid for NSD (non single diffractive) collisions in full phase space up to SppS energies ($\sqrt{s}$ = 200 GeV). For limited $\eta$-intervals it still remains valid at LHC energies [16, 25]. Negative binomial distributions (NBDs) describe multiplicity distributions well, a fact which is theoretically not well understood. Cluster models which assume an independent emission of clusters followed by stimulated particle emission within a cluster lead to multiplicity distributions of NBD type. NBDs describe multiplicity distributions of NSD collisions in full phase space up to $\sqrt{s}$ = 900 GeV where deviations have been observed. In limited $\eta$-intervals the description still holds at LHC [25, 26]. The combination of two NBDs, one representing soft and the other semi hard events (defined as events with and without minijets, respectively) describes multiplicity distributions up to the highest measured energy in full phase space (1.8 TeV) and in limited phase space intervals also at the LHC. The identification of trends of the fit parameters turns out to be ambiguous and assumptions are needed to obtain a coherent picture.

Although no sound theory arguments exist at present why multiplicities in pp and $e^+e^-$ collisions should behave similarly, the average multiplicities as function of $\sqrt{s}$ are similar when the concept of effective energy is introduced: $E_{\rm eff} = \sqrt{s} - E_{\rm lead,1} - E_{\rm lead,2}$ where $E_{\rm lead,i}$ is the energy which is retained by the proton remnants. The available energy for particle production is characterized by the inelasticity $K = E_{\rm eff}/\sqrt{s}$. This concept allows one to fit the average multiplicity in pp collisions with the following form: $f_{\rm pp}(\sqrt{s}) = f_{\rm ee}(K\sqrt{s}) + n_0$. $n_0$ is the contribution of the leading protons to the total multiplicity. One obtains a good fit result with $K = 0.35$ and $n_0 = 2.2$, i.e., about one third of the energy is available for particle production compared to $e^+e^-$ collisions. Phenomenologically, one

could ask if this is a hint that only one out of the three valence quarks is available for particle production. However, the similarity between pp and $e^+e^-$ collisions cannot be found in more differential distributions, e.g. in (pseudo)rapidity densities.

Results from LHC show a faster increase of the average multiplicity than anticipated by models [26, 27]. In particular phenomenological extrapolations and MCs with pre-LHC tunes underpredict the results at 7 TeV. Updated tunes which include LHC data indicate that parameters governing the amount of multiple-parton interactions need to be modified to reproduce the LHC multiplicities.

**LHCb QCD results**

*Sebastian Schleich*[3] *(TU Dortmund)*

The Large Hadron Collider (LHC) delivered data in proton-proton collisions at unprecedented center of mass energies of $\sqrt{s}$ = 900 GeV and 7 TeV, which allow one to test quantum chromodynamics (QCD) predictions in both, the perturbative and the non-perturbative regime. For example, the hadronization process falls into the latter. Predictions of the hadronization are based on phenomenological models, that are mostly tuned on LEP data and their validity under LHC conditions needs to be confirmed by experiments. Designed for precision measurements in the B meson system, the Large Hadron Collider beauty (LHCb) experiment [28] has several features that account for unique opportunities for QCD studies in proton-proton collisions at the LHC: It covers a large forward rapidity range of $1.9 < \eta < 4.9$. Further, its tracking system includes a silicon tracker in close vicinity to the proton-proton interaction point and the experiment is equipped with a dedicated particle identification system based on two ring imaging Čerenkov detectors.

The $K_S$ production cross section measured at $\sqrt{s} = 900$ GeV in the kinematic region $(p_T <$ 1.6 GeV/c) $\times (2.5 < y < 4.0)$ is found [29] to be in agreement with the Monte Carlo prediction (PYTHIA 6.4, Perugia 0 tune [30], in the following referred to as MC), the $p_T$ spectrum tends to be slightly harder on data as compared to MC. Not as good agreement is found in inclusive $\phi$ production cross section studies[4] at $\sqrt{s} = 7$ TeV. The measured production cross section in the kinematical range (0.8 GeV/c $< p_T <$ 5 GeV/c) $\times (2.44 < y < 4.06)$ is significantly enhanced with respect to MC, where also the $p_T$ spectrum is harder on data than on MC.

The baryon suppression in $\bar{\Lambda}/K_S$ is a sensitive test of fragmentation models because the initial state is purely baryonic. Similar considerations hold for particle-antiparticle ratios, since they probe the baryon transport from the beam to the final state. The particle ratio measurements $\bar{\Lambda}/K_S$, $\bar{\Lambda}/\Lambda$ and $\bar{p}/p$ are presented at both, $\sqrt{s} = 900$ GeV and 7 TeV. The $\bar{\Lambda}/K_S$ ratio is underestimated by MC at both beam energies. In contrast, the $\bar{\Lambda}/\Lambda$ ratio in the kinematical range $2 < y < 4$ is significantly overestimated by MC at $\sqrt{s} = 900$ GeV, whereas at 7 TeV the data is in better agreement, but still slightly lower than MC. The $\bar{p}/p$ ratio, measured in the range $2.8 < y < 4.5$, is slightly lower on $\sqrt{s} = 900$ GeV data than on MC, whereas it is in rather good agreement at 7 TeV. The hard QCD measurements presented are the Drell-Yan muon production $p_T$ spectrum at $\sqrt{s} = 7$ TeV, which is found to be in good agreement with the Monte Carlo prediction based on MCFM NLO. Additionally, the lepton $p_T$ spectrum in in the $W \to \mu\nu$ decay, as well as the charge asymmetry versus lepton pseudorapidity in this decay channel is presented. The results presented, still based on a relatively small data sample (59 $nb^{-1}$), are in agreement with Monte Carlo predictions within their statistical uncertainties.

[3] On behalf of the LHCb collaboration.

[4] All results, except for the $K_S$ cross section at $\sqrt{s} = 900$ GeV are preliminary

**First TOTEM results and perspectives**

*Karsten Eggert*[5] *(CERN & Cleveland)*

TOTEM is a dedicated experiment focused on forward physics complementary to the programmes of the large general-purpose experiments at the LHC [31]. TOTEM will measure the total proton-proton cross-section with the luminosity independent method based on the Optical Theorem which requires a detailed study of the elastic scattering cross-section down to a squared four-momentum transfer $|t|$ of $10^{-3}$ GeV$^2$ and the measurement of the total inelastic rate. Furthermore, TOTEM's physics programme aims at a deeper understanding of the proton structure by studying elastic scattering at large momentum transfers, and via a comprehensive menu of diffractive processes. To perform these measurements, TOTEM requires a good acceptance for particles produced at very small angles with respect to the beam. The coverage in the pseudorapidity-range of $3.1 < |\eta| < 6.5$ ($\eta = -\ln\tan\theta/2$) on both sides of the intersection point is accomplished by two telescopes for inelastically produced charged particles and complemented by Silicon detectors in special movable beam-pipe insertions – so called Roman pots (RP) – placed at about 147 m and 220 m from the interaction point, designed to detect leading protons at merely a few mm from the beam centre.

During the year 2010, TOTEM has participated at the normal low-$\beta^\star$ high-intensity runs with the vertical RP detectors at a distance to the beam of $18\sigma$ and the horizontal at $20\sigma$. With this configuration, large-$t$ elastic scattering could be measured for $t$- values above 2.2 GeV$^2$. Furthermore, Single Diffraction and Double Pomeron processes were detected over a large region in the ($\xi = \Delta p/p$, $t$) plane and correlations between the forward proton and the particle densities in the very forward inelastic detectors are studied as a function of $\xi$. In addition, data were taken with only a few bunches during TOTEM dedicated runs where the vertical Roman Pots have been moved closer to the beams ($7\sigma$) and a low intensity bunch with $10^{10}$ protons, to reduce pile-up, was added. Out of this data sample of several million events, 80k elastic scattering events with $t$-values above 0.4 GeV$^2$ were extracted. The $t$-distribution showed the usual exponential slope at low $t$, but also exhibits a clear diffractive dip at around 0.6 GeV$^2$, as it was observed for the first time at the ISR, whereas proton-antiproton elastic scattering only showed a shoulder in the $t$-distribution. The combination of these dedicated runs with the standard high-intensity runs will allow TOTEM to measure the $t$-distribution in the range of 0.4 - 4 GeV$^2$ and to distinguish between the various models on the market. The low intensity bunch with a reduced pile-up of about 1% is used to measure the forward charged multiplicity and forward-backward multiplicity correlations. During the year 2011, TOTEM will concentrate on the total cross-section measurement, which becomes possible with the presently installed inelastic Cathode-Strip-Chambers. However, a special beam optics with large $\beta^*$ around 90 m has to be developed to enable the measurement of sufficiently small $t$-values necessary for the extrapolation to the optical point. Furthermore, the extensive studies of the forward particle flow and diffractive topologies will continue.

**LHCf results**

*Massimo Bongi*[6] *(Universita & INFN, Firenze)*

LHCf is an LHC experiment designed to study the very forward production of neutral particles in $pp$ collisions. Its results can provide valuable information for the calibration of the hadron interaction models used in Monte Carlo simulation codes, aiming in particular to clarify the interpretation of

[5]On behalf of the TOTEM collaboration.

[6]On behalf of the LHCf collaboration.

the energy spectrum and the composition of high energy cosmic rays as measured by air-shower experiments. The highest-energy data currently available for the forward neutral-pion production spectrum reach $\sqrt{s} = 630$ GeV (UA7 experiment [32] operated at the Sp$\bar{p}$S in 1985-1986). The LHCf set-up consists of two imaging calorimeters (Arm1 and Arm2) symmetrically placed 140 m away on both the sides of the ATLAS interaction point, covering the pseudorapidity range $|\eta| > 8.4$. Further information about the scientific goal, the technical details and the performance of the detectors can be found in the following references: [33–39]. The experiment has successfully finished taking $pp$ data at $\sqrt{s} = 0.9$ TeV and at $\sqrt{s} = 7$ TeV in 2009-2010. A preliminary analysis of the energy spectra of $\gamma$-ray like and hadron like events measured by the calorimeters (Arm1 - upper plots, Arm2 - lower plots) at $\sqrt{s} = 0.9$ TeV, compared with the expectation of MC simulations, are shown in the Fig. 3. Only statistical errors are reported and simulations are normalized by total entries of $\gamma$- and hadron-like events. The detectors were removed in July 2010 for an upgrade which will improve their radiation hardness, and they will be back in the LHC tunnel for the collisions at $\sqrt{s} = 14$ TeV.

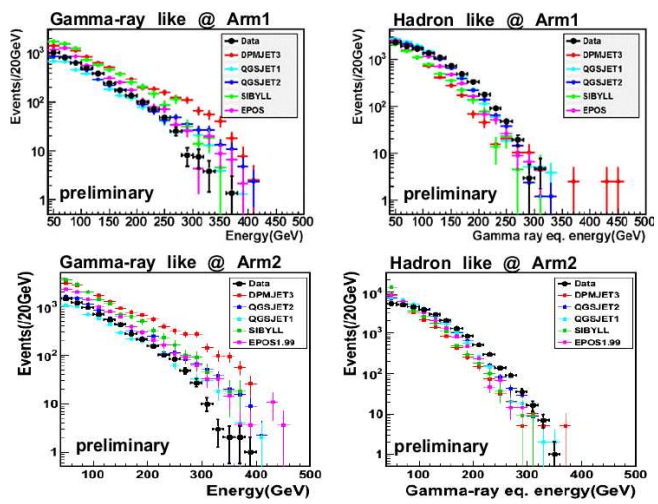


Figure 3: Energy spectra of $\gamma$- and hadron-like events measured by LHCf Arm1 (top) and Arm2 (bottom) in $pp$ at $\sqrt{s} = 0.9$ TeV compared with MC simulations.

**Tevatron results of relevance for cosmic-rays**

*Lars Sonnenschein*[7] *(RWTH Aachen)*

The two multi-purpose experiments DØ [40] and CDF [41] are operated at the Tevatron collider, where proton anti-proton collisions take place at a centre of mass energy of 1.96 TeV in Run II. In the kinematic plane of $Q^2$-scale and (anti-)proton momentum fraction $x$, Tevatron jet measurements cover a wide range, with phase space regions in common and beyond the HERA $ep$-collider reach. The kinematic limit of the Auger experiment is given by a centre of mass energy of about 100 TeV. Cosmic rays cover a large region of the kinematic phase space at low momenta $x$, corresponding to forward proton/diffractive physics and also at low scales, corresponding to the hadronisation scale and the underlying event. Therefore of particular interest are exclusive and diffractive measurements as well as underlying event, double parton scattering and minimum bias measurements. The kinematic limit of the Tevatron corresponds to the PeV energy region below the knee of the differential cosmic particle flux energy distribution. The data discussed here are in general corrected for detector effects,

[7] On behalf of the CDF and DØ collaborations.

such as efficiency and acceptance. Therefore they can be used directly for testing and improving existing event generators and any future calculations/models. Comparisons take place at the hadronic final state (particle level).

In particular for elastic and exclusive production measurements [42,43] forward proton detectors, which cover a pseudorapidity range of up to $|\eta| \lesssim 8$ and momentum fractions of $0.03 < \xi \lesssim 0.10$ are useful, to detect the intact (anti-)proton. Many further analyses of exclusive and diffractive production [44–50] have been accomplished. Underlying event, double parton scattering and minimum bias studies have been addressed by the measurements [51–56]. The studies have been pioneering work in many cases. Methods have been established which are widely used by LHC experiments today. The measurements have provided very important input to theorists, in particular with respect to non-perturbative QCD physics, where phenomenological models are varying considerably. Most prominently the breakdown of factorisation between HERA and Tevatron has been established [46]. The double Pomeron exchange mechanism offers the possibility to study the exclusive Higgs production at the LHC, where predictions did vary by a factor of 1000 before the CDF measurement [46]. Already in Run I CDF has provided useful input for diffractive parton distribution functions.

**QCD results from HERA**

*Armen Bunyatyan*[8] *(Yerevan & DESY)*

New QCD results obtained by the H1 and ZEUS experiments at HERA collider are reviewed. These results are based on data taken in $e^{\pm}p$ collisions during 1994-2007 corresponding to an integrated luminosity of almost 0.5 fb$^{-1}$ for each experiment. HERA provides unique information on the proton structure. High center of mass energy $\sqrt{s} = 320$ GeV gives access to both the low Bjorken-$x$ domain and regime of high momentum transfers squared $Q^2$. An ultimate precision of DIS cross section measurement is achieved by combining the H1 and ZEUS measurements. The combined data are used as a sole input to a QCD fit to obtain HERAPDF sets. Important cross checks of the conventional QCD picture and the additional constraints for the gluon density distribution in the proton are provided by the measurements of the structure function $F_L$ and the charm and beauty cross sections. New measurements of inclusive neutral and charged current scattering cross sections at high $Q^2$ improve precision in this kinematic domain. Jet production at HERA provides an important testing ground for pQCD and new constraints for the gluon density distribution in the proton. The running of strong coupling $\alpha_S$ is demonstrated and its value at $Z^0$ mass, $\alpha_S(M_Z^0)$, is determined from the jet measurements at HERA with high precision.

The cross section of inclusive DIS diffractive process is measured within a wide kinematic range. The diffractive parton distribution functions (DPDFs) of the proton are determined from QCD fits to the data including the dijet production cross sections in diffractive DIS. Predictions based on these DPDFs are in agreement with the measured cross section of diffractive dijet and charm production in DIS at HERA and the longitudinal diffractive structure function $F_L^D$.

Data from the recent measurements of leading proton and neutron production are presented and compared to the theoretical models. The measurements are well described by the models which include the baryon production via virtual meson exchange. The leading proton and neutron data from the H1 and ZEUS experiments are also compared with the hadron interaction models which are used in the analyses of ultra-high energy cosmic rays. The sensitivity of the HERA leading baryon data to the differences between the models is demonstrated.

[8] On behalf of the H1 and ZEUS collaborations.

**Performance of the ALICE experiment for cosmic ray physics**

*Bruno Alessandro*[9] *(INFN, Torino)*

A large number of atmospheric muon events were recorded during 2009 and 2010 for the calibration, alignment and commissioning of most of the ALICE (A Large Ion Collider Experiment at the CERN LHC) detectors. In this Workshop we presented the analysis of some of these data to understand the performances and the possibilities of ALICE to study topics connected to cosmic ray physics. The ALICE central detectors select atmospheric muons with zenith angle in the range $0^\circ - 60^\circ$. The muons are tracked in a large volume Time Projection Chamber (TPC) that measures the muon multiplicity, and for each muon the momentum, the sign, the direction and the spatial coordinates. An analysis of these observables and some correlation among them have been presented. In particular the muon multiplicity distribution and some events with very high multiplicity have been shown and detailed analyzed. A first attempt to measure the ratio $\mu^+/\mu^-$ for vertical muons ($0^\circ - 20^\circ$) with a limited statistics has been presented and compared with world previous measurements.

Horizontal muons, that is muons with zenith angle in the range $60^\circ - 90^\circ$ are very rare events that have been detected by the Forward Muon Spectrometer in 9 days of data taking. A selection of these events to obtain a good sample to measure the momentum distribution and the ratio $\mu^+/\mu^-$ at surface level has been discussed and measurements shown.

**CMS results on forward physics and other of relevance for cosmic rays**

*Lev Kheyn*[10] *(MSU, Moscow)*

Evidences of observation of single-diffraction at the LHC are presented at 900 and at 2360 GeV. Single-diffractive events appear as a peak at small values of the variable $E \pm pz$ which is proportional to $\xi$, the proton fractional energy loss, reflecting the $1/\xi$ behaviour of the diffractive cross section. Single-diffractive events also appear as a peak in the energy distribution of the forward calorimeter HF, reflecting the presence of a rapidity gap over HF. The data have been compared on the detector level to PYTHIA 6 and PHOJET generators. PYTHIA 6 gives a better description of the non-diffractive component of the data, while PHOJET reproduces the diffractive contribution more accurately.

The energy flow (at detector level) for minimum bias events and events having a hard scale defined by a dijet with $E_{T,jet}$ >8 GeV ($E_{T,jet}$ >20 GeV for $\sqrt{s}$ = 7 TeV) in $|\eta| < 2.5$ has been measured for the first time in hadron-hadron collisions in the forward region of $3.15 < |\eta| < 4.9$. The increase in energy flow in the forward region with increasing centre-of-mass energy is significant and is reproduced by Monte Carlo (MC) simulations for events with dijets, whereas it is underpredicted for minimum bias events. None of the MC simulations manages to describe all energy flow data. Monte Carlo tunes which are closer to the measurements for minimum bias events differ from measurement in dijet events. Particularly for minimum bias events, the measured energy flow at $\sqrt{s}$ = 7 TeV is larger than any of the predictions. Those MC simulations which best describe the energy flow in the forward region are different from those which best describe the complementary measurements of charged particle spectra in the central region. The measurement of the energy flow in the forward region therefore provides further input to the tuning of MC event generators and it constrains modelling of multiple interactions at high energies. CMS measurements of charged particle pseudorapidity densities are being compared with cosmic ray (CR) generators. The distribution proves of high discriminative power, revealing large spread of the CR MCs predictions at highest energy of 7 TeV.

[9] On behalf of the ALICE collaboration.

[10] On behalf of the CMS collaboration.

The flux ratio of positive- to negative-charge cosmic muons has been measured as a function of the muon momentum and its vertical component. This is most precise measurement below 100 GeV. The ratio was measured over broad range 10 GeV - 1 TeV of transition from approximately constant to a rising value.

**STAR results of relevance for cosmic rays**

*Joanna Kiryluk*[11] *(LBL, Berkeley)*

The Relativistic Heavy Ion Collider (RHIC) is a versatile accelerator situated at Brookhaven National Laboratory which commenced operations in 2000. It collides heavy ions as well as polarized protons at center of mass energies of up to 200 GeV per nucleon and 500 GeV, respectively. The Solenoid Tracker At RHIC (STAR) detector [57] provides tracking, particle identification, and electromagnetic calorimetry covering large acceptance. Key strengths include the capability to reconstruct jets, study correlations, and identify particles in high multiplicity environments.

Measurements in unpolarized $pp$ collisions at RHIC test perturbative QCD (pQCD) calculations. The data on jet and inclusive particle production cross sections [58, 59] are in good agreements with Next-to-Leading-Order (NLO) pQCD calculations. Recent measurements of the $W^{\pm}$ boson production in 500 GeV $pp$ collisions at RHIC and in 7 TeV collisions at the LHC are in good agreement with NLO pQCD over a wide range in $\sqrt{s}$ [60].

The flux of prompt leptons at the Earth is of importance to cosmic ray (CR) and neutrino physics. Estimates depend strongly on models for the charm cross section and energy spectra. These models use the pQCD framework and extrapolate charm collider data to CR energies. The flux of prompt leptons is strongly dependent also on the small-$x$ nuclear gluon distributions. New dynamical effects, such as parton saturation that may be observed at forward collider rapidities, change the DGLAP dynamics and thus the flux estimates [61]. STAR and PHENIX data [62] on electrons from heavy-flavor decays are consistent in the regions of kinematic overlap and are well described by Fixed-Order-Next-to-Leading Logarithm calculations [63]. The STAR J/$\Psi$ data [64] are well-reproduced by calculations [65] using the color octet and singlet models in non-relativistic QCD. STAR has determined the B-hadron feed-down contribution to the inclusive $J/\Psi$ yield from $J/\Psi$-hadron azimuthal angle correlations. It is found to be 10-25% and has no significant $\sqrt{s}$ dependence from RHIC to LHC energies [66]. The STAR $\Upsilon$(1S+2S+3S) production cross section [67] is consistent with world data and NLO pQCD calculations in the Color Evaporation Model [68].

Collisions of $dAu$ ions at $\sqrt{s_{NN}} = 200$ GeV at RHIC have made it possible to study the modification of elementary QCD processes in cold nuclear matter (CNM), and provide insight in coherence effects or shadowing in nuclei, the saturation of small-$x$ gluons, parton energy loss, and soft multiple scattering effects. Forward particle production is found to be suppressed [59, 69] and back-to-back correlations are reduced [70], consistent with saturation models [71]. Hot matter effects have been studied at RHIC in $AuAu$ collisions. The observation of phenomena such as jet quenching and collective motion suggests that a thus far unobserved state of hot and dense matter with partonic degrees of freedom, resembling an ideal and strongly-coupled fluid, has been created [72]. The ongoing Beam-Energy Scan program aims to observe the anticipated critical point in the QCD phase diagram [73]. STAR has also observed anti-hypertriton production in $AuAu$ collisions [74], the first ever observation of an anti-hypernucleus. The production and properties of antinuclei, and nuclei containing strange quarks, have implications spanning nuclear and particle physics, astrophysics, and cosmology.

[11] On behalf of the STAR collaboration.

# 2 Hadronic collisions at multi-TeV energies: Theory

### Monte Carlo tuning at the LHC

*Holger Schulz*[12] *(Inst. für Phys., Humboldt-Univ. Berlin)*

Monte Carlo simulations of high energy physics processes are essential for many aspects of the LHC physics programme, e.g. the experiments use them to determine backgrounds to signal processes and to estimate reconstruction efficiencies, which are sources of systematic uncertainties that clearly dominate over statistical errors at the LHC. In order to reduce these systematic uncertainties, proton-proton collisions need to be simulated in such a way that they look as close to real data as possible. This however can in many cases only be achieved by optimising phenomenological model parameters to data, especially when 'soft' QCD effects such as multiple parton interactions or hadronisation are to be described.

An overview of such parameter tuning strategies currently applied at the LHC has been presented, i.e. conventional manual parameter optimisation by the CMS collaboration and systematic tunings within ATLAS. The focus was clearly on the latter, where the software packages Professor and Rivet that allow for a systematic tuning effort using statistical techniques are used extensively.

Rivet is an application that reads in generator independent events ("HepMC" format), processes these events by applying user written routines that mimic actual data analyses. After processing the generated events, histograms are produced that use the same binning as published data.

Running a Monte Carlo event generator can be regarded as calculating a very expensive function. The key feature of Professor is the parameterisation of this expensive function by means of parameterisations using polynomials such that one effectively produces a fast analytic model of the Monte Carlo generator response to shifts in parameter space. It is thus possible to get a very good approximate description of a generator at a certain point in parameter space in less than a second; a task that takes hours or even days with conventional methods. With this fast model, the task of tuning parameters is therefore passed on to constructing a goodness-of-fit measure between the parameterised generator response and real data. In this context, the necessity to have data, corrected for detector effects has been stressed.

Further uses of the parameterisation like calculating the sensitivity of observables to shifts in parameter space and an interactive Monte Carlo simulator ("prof-I") have been presented. The successful usage of Professor and Rivet has been illustrated by recent tunings performed within the ATLAS collaboration. Examples have been given ("AMBT1", "AUET1") and it has been stressed how fast the turn-around from taking new data to getting new tunings that include these data can be. Also, more special uses of Professor to study systematic variations ("Eigentunes", re-tuning using different PDFs) have been presented.

### Parton correlations and fluctuations

*Gösta Gustafson*[13] *(Lund University)*

Multiple interactions and diffraction are important components in high energy collisions [75, 76]. These effects are influenced by correlations and fluctuations in the parton evolution, and the understanding of these features is therefore essential for a proper interpretation of data from LHC and

[12] On behalf of the Professor and Rivet collaborations.

[13] In collaboration with C. Flensburg, L. Lönnblad, and A. Ster.

cosmic ray experiments. At high energies parton distribution functions at very small $x$-values are governed by BFKL dynamics and saturation effects are important. Mueller's dipole model is a formulation of LL BFKL evolution in transverse coordinate space. The Lund Dipole Cascade model is a generalization of Mueller's model, which also includes non-leading effects from *e.g.* energy-momentum conservation and running coupling, saturation effects in the cascade evolution, and confinement. The model is implemented in a MC called DIPSY, and in this talk I use it to study effects of correlations and fluctuations on double parton interactions and diffraction.

In parton evolution à la BFKL the gluons are strongly correlated. An analysis of double parton distributions shows increased correlations for small $x$ and large $Q^2$. A spike develops for small separations between the partons in transverse coordinate space. The correlation can also be expressed in terms of an "effective cross section", which becomes reduced at high energies and large $p_\perp$.

In the Good–Walker formalism diffractive excitation is determined by the fluctuations in the scattering amplitude between different components in the projectile wavefunction. In BFKL the proton substructure in terms of a parton cascade has large fluctuations and can fill a large rapidity range. An analysis of these fluctuations reproduces low and high mass diffractive excitation in DIS and $pp$ collisions. For $pp$ scattering the fluctuations are suppressed by unitarity constraints, which leads to a breaking of factorization between DIS and $pp$.

The model can also be applied to nuclear collisions, and finally I present some preliminary results for exclusive final states in $pp$, $pA$, and $AA$ collisions.

**A new model for minimum bias and the underlying event in SHERPA**

*Korinna Zapp*[14] *(Durham)*

Minimum bias events reveal not only the most complete view on the physics at hadron colliders, but also have an intimate connection to the underlying event and are thus highly relevant to many high-$p_\perp$ processes. Higgs searches at the LHC, for instance, rely largely on event topologies with rapidity gaps. The feasibility of such measurements depends strongly on the survival probability of rapidity gaps. Apart from the connection to the underlying event, diffraction as an important part of minimum bias events is interesting in its own right.

Unfortunately, no model describing soft, semi-hard, diffractive and hard QCD events has been implemented in a multi-purpose event generator so far. The Khoze-Martin-Ryskin model [77] is a multi-channel eikonal model that by summing all multi-pomeron diagrams is capable of describing elastic and inelastic scattering, low mass and high mass diffractive dissociation and central exclusive production.

The Monte Carlo realisation relies on the partonic interpretation of the model. The simulation of elastic scattering is straight-forward, while the inelastic collisions are more involved. First, the number of exchanged ladders and the impact parameters of the ladders have to be generated. The emissions from the ladder are generated using a Sudakov form-factor, that accounts for absorptive corrections and Regge dynamics. The colour charge of the $t$-channel propagators has to be fixed, the singlet exchanges naturally give rise to rapidity gaps. Finally, the hardest emissions are corrected to pQCD matrix elements to reproduce the correct high energy behaviour. The model will be formulated also as a model for the underlying event and become available as part of the SHERPA 1.3 release.

[14] In collaboration with H. Hoeth, V. Khoze, F. Krauss, A. Martin and M. Ryskin

**Multiple partonic interactions with HERWIG++**

*Stefan Gieseke (ITP, Karlsruhe)*

The focus of this talk is on the development of a multiple partonic interaction (MPI) model for minimum bias interactions and the underlying event in HERWIG++. We briefly summarize the general purpose Monte Carlo event generator HERWIG++ [78–81] before describing the development of the MPI model [82–84] in detail. We explain the relevance of the main parameters of our model, the inverse radius $\mu^2$ and $p_T^{\min}$ in detail. The former characterizing the width of the spatial transverse parton distribution inside a hadronic projectile and the latter the transverse momentum down to which a partonic interaction will still be described by perturbative QCD. The development of the model was done in several steps which are briefly explained.

1. A semi hard model for MPI, containing only interactions above $p_T^{\min}$ [85, 86].
2. A soft model, also for interactions below $p_T^{\min}$ [87–89].
3. An extension of the model to allow for colour reconnections [90].

The final model is shown to describe data from CDF [91, 92] and recent non–diffractive minimum bias and underlying event data from ATLAS at 900 GeV and 7 TeV [5, 7, 93]. The residual energy dependence of the model parameters is briefly discussed and an outlook to further work on this dependence is given.

**PYTHIA 8 status**

*Torbjörn Sjöstrand (Lund University)*

The PYTHIA 8 event generator [94] is the C++ successor to the Fortran-based PYTHIA 6 [95], frequently used in the study of $pp/p\bar{p}$ and $e^+e^-$ physics. One of the main developments is that PYTHIA 8 now contains a complete interleaving of multiparton interactions, initial-state radiation and final-state radiation, in one common sequence of decreasing $p_\perp$ scales. That is, the features at larger $p_\perp$ values set the stage for the subsequent dressing-up by softer emissions. The approximate matching of showers to hard-scattering matrix elements has been improved for a large set of hard processes [96]. For showers in QCD processes the first emission is compared with $2 \to 3$ matrix elements to confirm a reasonable rate [97].

The traditional multiparton interactions framework is largely retained, but some new possibilities are added. One is that it is now possible to preselect two separate hard processes in the same event, to help simulate signals for double parton scattering. Another is that rescattering, where one parton scatters twice (or more) against partons from the other hadron, can now be simulated [98]. Unfortunately it is not simple to find a good experimental signal for such events. Other developments include an improved framework for the structure of diffractive events, a richer mix of underlying-event processes, and an updated set of parton distributions.

Early attempts to tune PYTHIA 8 to minimum-bias data gave too much underlying-event activity. The problem has been traced to a double counting between some initial- and final-state radiation. This has now been fixed, and tunes to Tevatron data have been produced [97]. Unfortunately these tunes underestimate the activity observed in some of the early LHC data sets, which either may be owing to problems with the generator not reproducing different cut conditions, or point to some tension in the data. For now a slightly separate LHC tune has been made.

PYTHIA 8 does not reproduce the CMS ridge effect, which thus shows that some physics mechanisms are still missing. Similarly there are problems e.g. with the particle composition and Bose-Einstein effects observed at LHC, that hints towards collective effects.

**Total hadronic cross sections at high energy**

*Rohini Godbole*[15] *(CTS-Bangalore & CERN))*

Energy dependence of total hadronic cross-sections is an important subject, both from a theoretical point of view due to its intimate relation to the non perturbative QCD dynamics and also from a phenomenological point of view, in the context of making accurate predictions for high energy cosmic ray interactions based on the currently available information. In this talk I present a summary of the current state of data and model predictions for the same, paying particular attention to the Eikonalised Minijet Model (EMM) supplemented with soft gluon resummation [99], which tames the unacceptably strong energy rise of the EMM.

The $pp, p\bar{p}$ and $\gamma p$ ($\gamma\gamma$) cross sections, scaled by a VMD inspired factor of 330 ($(330)^2$), all in fact show an almost universal behaviour, perhaps with a slightly faster rise for the $\gamma\gamma$ induced processes [100]. The models have to provide an explanation of the initial fall, normalisation at (and the position of) the minimum and the subsequent rise. The important issue to be addressed is the dynamics responsible for this rise, consistent with the Froissart bound. Then one can investigate the impact of these model predictions, extrapolated to cosmic ray energies. There exist different set of *fits* to the current data on total cross-sections, some of them with a form chosen so that various constraints from unitarity and analyticity are automatically satisfied. These have been then normally used to obtain the predicted total cross-sections at high energies.

In the EMM models the rise of cross-section with energy is driven by the minijet cross-section calculated in perturbative QCD (pQCD), its rise with energy given by $\sigma_{minijet} \propto \frac{1}{p_{tmin}^2}\left[\frac{s}{4p_{tmin}^2}\right]^{\varepsilon}$ where $\varepsilon = J-1$, $J$ being the degree of singularity of the gluon density in the proton. This has to be embedded in an eikonal formulation, which guarantees unitarity. The eikonalisation involves transverse parton overlap function in the two hadrons $A\&B$, $A_{AB}(\beta) = \int d^2b_1 \rho_A(\vec{b_1})\rho_B(\vec{\beta}-\vec{b_1})$. This, along with the minijet (and some parametrisation of soft) cross-section, then is used in building the total cross-section, $\sigma^{\rm tot}_{pp(\bar{p})} = 2\int d^2\vec{b}[1-e^{-n(b,s)/2}]$, with $n(b,s) = A_{AB}(b,s)\sigma(s)$.

Different EMM models differ in the way $A_{AB}(b,s)$ is modeled. In the GGPS model [99], the energy dependent transverse space matter distribution is calculated as the Fourier Transform of the transverse momentum distribution of the partons, which is built through resummation of soft gluon emissions from the valence quark in the proton (to the leading order in $\alpha_s(Q^2)$) [101]. In this BN EMM formulation, one of the important factor affecting the $\sigma^{\rm tot}$ is behaviour of $\alpha_s(Q^2)$ in the far infrared which is modeled by a form such that, $\alpha_s(k_T^2) \to (1/k_T^2)^p$ as $k_T^2 \to 0$. The requirement that our form of $\alpha_s$ be consistent with a confining potential and the singularity is integrable gives $1/2 < p < 1$. Further, in the high energy limit, one can show $\sigma^{\rm tot} \simeq (\varepsilon \ln s)^{1/p}$ and thus a high energy behaviour consistent with Froissart bound attains in our model naturally. Prediction of $\sigma_{\rm tot}$ over the whole energy range requires also the soft cross-section, $\sigma^{\rm soft}(s)$ and the corresponding overlap function $A_{AB}^{BN,soft}$, which are parameterised.

The left panel of Fig. 4 taken from Ref. [99], shows comparisons of a variety of model predictions with data and each other, the blue band corresponding to the spread in our fits. We see that the LHC

[15] In collaboration with A. Grau, G. Pancheri and Y. Srivastava.

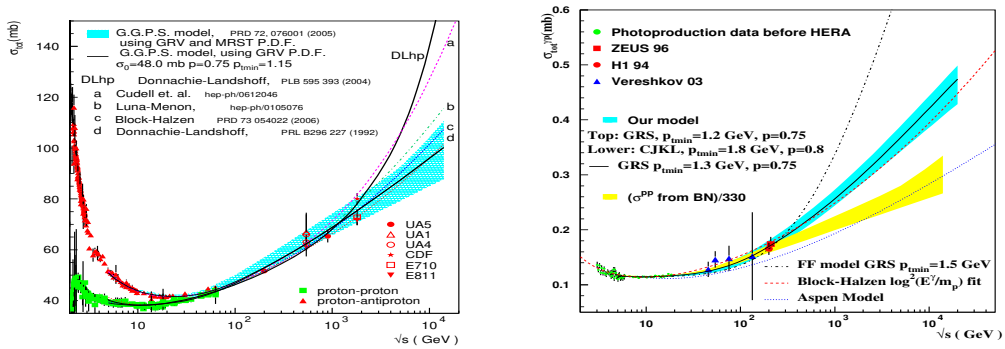


Figure 4: Predictions of the BN EMM [99] for $pp/p\bar{p}$ in the left panel and $\gamma p$ case [100] in the right panel, compared with different other model predictions as well as the data.

data will already offer us a nontrivial discrimination among the models. For the photon induced processes, the BN EMM has to be supplemented by one more parameter $P_{\rm had}$, the probability that the photon develops a hadronic structure. We find that the best fit seems to prefer a rise of $\gamma p$ cross-sections a little faster than the soft-pomeron predictions as well as those obtained, using factorisation, from our blue band for $\sigma_{\rm tot}^{pp}$ of the left panel. Of course now the interesting thing is to try and see the effect of these range of predictions of $\sigma_{\rm tot}^{pp/\bar{p}p}$ and the somewhat faster rise of the $\sigma_{\rm tot}^{\gamma p}$ on the cosmic ray simulations. Preliminary investigations [102], for a photon energy of $10^{19}$ eV, show that this difference can affect the development of the longitudinal profile of muonic showers by $\sim 10\%$.

The model has been recently applied to $\pi p$ and $\pi\pi$ cross-sections [103]. In these cases the energy ranges over which the data are available are rather limited and in the latter case even the onset of the rise is not clearly established. The LHC with zero degree calorimeter (ZDC) can in fact provide nontrivial information to increase our confidence in making predictions for collisions with cosmic ray energies. In conclusion, the different models for total cross-sections seem to be good shape. The QCD based BN-EMM, which uses the experimentally measured parton densities and ideas of soft gluon resummation, in fact is able to even predict the Froissart bound. The same model gives a consistent description of high energy $\gamma p$ data and can be extended to $\pi$ induced processes. The LHC data can play an important role in sharpening up our predictions so that they can be extended to the highest cosmic-ray energies.

**On strategies for determination and characterization of the underlying event**

*Sebastian Sapeta (LPTHE, Paris)*

The underlying event (UE) is a soft activity which accompanies each hard process studied at hadron hadron collider. Its good understanding is of great importance since the UE affects a wide variety of high-$p_T$ measurements, e.g. by introducing a bias or by degrading kinematic jet reconstruction. However, both an unambiguous definition of UE and its modeling faces a number of problems. Therefore, it is particularly important to be able to measure the UE as well as possible so that corresponding experimental results can be used as an input to further constrain the models.

We have carried out a twofold study devoted to this issue [104]. First, we asked the question of how the existing methods of UE determination perform on the practical aspects of the problem. Developing a simple toy model of UE and using is as a testing ground, we have examined two methods: the "traditional approach" [105] and the more recent area/median approach [106, 107]. One conclusion from this part of our study is that for determinations of averaged quantities, like the average

transverse momentum of UE per unit area in the (y,$\phi$)-plane, $\langle\rho\rangle$, both methods give comparably good results. In contrast, for event-by-event measurements and determinations of fluctuations of UE, the traditional approach is affected significantly more by the contamination coming from the hard part of the event.

The second question we studied was that which observables related to the energy flow of UE are interesting to measure. Here, we chose the area/median method to examine more realistic UE from the Monte Carlo (MC) models and found noticeable differences between predictions of different generators/tunes extrapolated to LHC energy. Therefore, we conclude that a broader range of observables deserves dedicated measurements. Those include rapidity dependence of $\rho$, intra- and inter-event fluctuations and correlations. A first step of this program has already bin made by the CMS collaboration which used the area/median approach to measure the charged component of the UE at $\sqrt{s} = 0.9$ TeV. The preliminary results [108] show that, even at low multiplicities, the method is capable to constraint MC tunes.

**Gluon saturation at the LHC from Color-Glass-Condensate**

*Amir Rezaeian (Valparaiso)*

At high energy, a system of parton (gluons) forms a new state of matter: Color-Glass-Condensate (CGC) [109]. The CGC is the universal limit for the components of a hadron wavefunction which is highly coherent and extremely high-energy density ensemble of gluons. In the CGC picture, the density of partons $\rho_p$ with a typical transverse momenta less than $Q_s$ reaches a high value, $\rho_p \propto 1/\alpha_s \gg 1$ ($\alpha_s$ is the strong coupling constant). The saturation scale $Q_s$ is a new momentum scale that increases with energy. At high energies/small Bjorken-$x$, $Q_s \gg \mu$ where $\mu$ is the scale of soft interaction. Therefore, $\alpha_s(Q_s) \ll 1$ and this fact allows us to treat this system on solid theoretical basis. On the other hand, even though the strong coupling $\alpha_S$ becomes small due to the high density of partons, saturation effects, the fields interact strongly because of the classical coherence. This leads to a new regime of QCD with non-linear features which cannot be investigated in a more traditional perturbative approach. In the framework of the CGC approach the secondary hadrons are originated from the decay of gluon mini jets with the transverse momentum approximately equal to the saturation scale $Q_s(x)$ [110]. The first stage of this process is rather under theoretical control and determines the main characteristics of the hadron production, especially as far as energy, rapidity and transverse momentum dependence are concerned. The jet decay and hadronization unfortunately, could be treated mostly phenomenologically.

The CGC [110] predicted 7 TeV data in $pp$ collisions [16] including (i) multiplicity distribution, (ii) inclusive charged-hadron transverse-momentum distribution, (iii) the position of peak in differential yield 4) average transverse momentum of the produced hadron as a function of energy and hadron multiplicity. The same model also describes $ep$, $eA$ and $AA$ (at RHIC) data in an unified fashion supporting the universality of the saturation physics. It has been shown that the observed ridge phenomenon in $pp$ collisions at the LHC can be also explained by the CGC [111]. There exists some ideas how to simulate the CGC state in $AA$ collisions due to higher density but evidence for the formation of the CGC state (gluon saturation) in proton-proton interaction will be a triumph of the high-density QCD and the CGC.

The physics of $AA$ collisions is more complicated compared to $pp(A)$ and $ep(A)$ collisions. The ALICE collaboration has recently released new data for the multiplicity in central $PbPb$ collisions at $\sqrt{s_{NN}} = 2.76$ TeV [112]. There are some surprises in the ALICE data: (i) the power-law behavior on energy in $AA$ is so different from $pp$ collisions which is not very easy to accommodate within the CGC approach, (ii) the models that describe DIS for proton, DIS for nucleus, the LHC data

for proton and RHIC data apparently failed to describe the ALICE data with the same accuracy. It appears apparently to be difficult to describe at the same time, HERA and RHIC and the new ALICE data for the multiplicity [113]. First notice that, the ALICE $0-5\%$ centrality bin at $\sqrt{s_{NN}} = 2.76$ TeV corresponds to $N_{part} = 381$ while our approach based on the Glauber model gives $N_{part} = 374$ [114]. Therefore, our actual prediction [114] for the same centrality bin will be higher than what the ALICE collaboration quoted in their paper [112]. Assuming that the ALICE data is correct, saturation models gave correct predictions for multiplicity in $AA$ collisions at the LHC within about less than 20% error. Indeed, this is not horribly bad given the simplicity of the approach. However, this will give rise to several open questions: (i) what is the role of final-state effects? (ii) how the mini-jet mas changes with energy/rapidity in a very dense medium?, (iii) what is the effects of fluctuations and pre-hadronization?. One should also have in mind that the $k_T$ factorization for $AA$ collisions has not yet been proven and gluon production in $AA$ collisions is still an open problem in the CGC. To conclude, the first LHC data for $AA$ collisions has already created much excitement in the heavy ion community and it opened a fresh and hot debate on how the saturation physics changes from $ep$, $pp$ and $eA$ to $AA$ collisions.

**Systematic study of inclusive hadron production spectra in collider experiments**

*Andrey Rostovtsev*[16] *(ITEP, Moscow)*

There exists a large body of experimental data on hadron production in high energy proton-(anti)proton, photon-proton, photon-photon and heavy ion collisions. In the present report the experimentally measured inclusive spectra of long-lived charged particles produced at central rapidities in the colliding particles center of mass system are considered. The analysed published data have been taken with a minimum bias trigger conditions and at center of mass energy $(\sqrt{s})$ ranging from 23 to 2360 GeV.

The charged particle spectra as function of transverse momentum are traditionally approximated using the Tsallis-type (power law) function. However, a closer look at the fits to the available data discloses systematic defects in this approximation. It is found, the parameterization

$$\frac{d\sigma}{p_T dp_T} = A_e \exp\left(-E_T^{kin}/T_e\right) + \frac{A}{(1+\frac{p_T^2}{T^2 \cdot n})^n} \tag{1}$$

is in much better agreement with the data then the Tsallis approximation. The variables in the equation above are self-explanatory. The most surprising feature of the new parameterization (1) is a strong correlation between the parameters $T_e$ and $T$. Though the physical origin of the observed correlation is not quite clear, it provides an additional constraint for the parameterization (1) and therefore reduces a number of free parameters. Interestingly, a similar combination of the Boltzmann-like and power-law terms is observed in the photon energy spectra from the sun flares.

The relative contributions of the terms in (1) are characterized by a ratio $R$ of the exponential to power law terms integrated over $p_T^2$. Interestingly, for $pp$ and $p\overline{p}$ data this ratio $R$ is almost independent of the collision energy and equals to about 4, while for $AuAu$ it reaches minimum values (about 2) at medium centralities of heavy ion collisions. In addition, in the high energy DIS, photoproduction and $\gamma\gamma$ collisions the power law term of the new proposed parameterization (1) dominates the produced particle spectra. Thus, only the inclusive spectra of charged particles produced in pure baryonic collisions require a substantial contribution of the Boltzmann-like exponential term.

[16] In collaboration with A. Bylinkin.

Finally, a map of the parameters $T$ and $n$ for proton-(anti)proton, heavy ion, γ-proton and γγ collision at different energies is drawn. There are two clearly distinct trends seen on the map. The $pp$ and $p\overline{p}$ collision data show an increase of the $T-$parameter and decrease of the $n$ parameter with collision energy $\sqrt{s}$ increasing. The second trend, where the values of both parameters the $T$ and $n$ increase, is defined mainly by the RHIC $AuAu$ collision data at $\sqrt{s_{NN}} = 200\ GeV$ per nucleon. In this case a simultaneous increase of the $T$ and $n$ values corresponds to an increase of the centrality of heavy ion collisions. Surprisingly, the both trends cross each other at medium centralities corresponding to the minimum bias $AuAu$ collisions and $p\overline{p}$ interactions with energy of $\sqrt{s_{NN}}$=200 GeV. Naively one could expect the single $p\overline{p}$ interaction has more similarity to the very peripheral single nucleon-nucleon interactions. Contrary to that, DIS, γ$p$ and γγ interactions belong to the second trend and are located on the parameter map nearby very peripheral heavy ion interactions at about the same collision energy per nucleon. A more extended version of this report can be found in [115].

**Hyperon transverse momentum distributions in $pp$ and $p\bar{p}$ collisions**

*Olga Piskounova (Lebedev Inst., Moscow)*

The analysis of data on hyperon transverse momentum distributions, $dN/dp_T$, that were gathered from various experiments (WA89, ISR, STAR, UA1 and CDF) reveals an important difference in the dynamics of multiparticle production in proton-proton vs. antiproton-proton collisions in the region 0.3 GeV/c $< p_T <$ 3 GeV/c. Hyperons produced with proton beams display a sharp exponential slope at low $p_T$, while those produced with antiproton beam do not. Since LHC experiments have proton projectiles, the spectra of multiparticle production at the LHC [27] should be "softer" in comparison to predictions, because the MC predictions were based on Tevatron (antiproton) data.

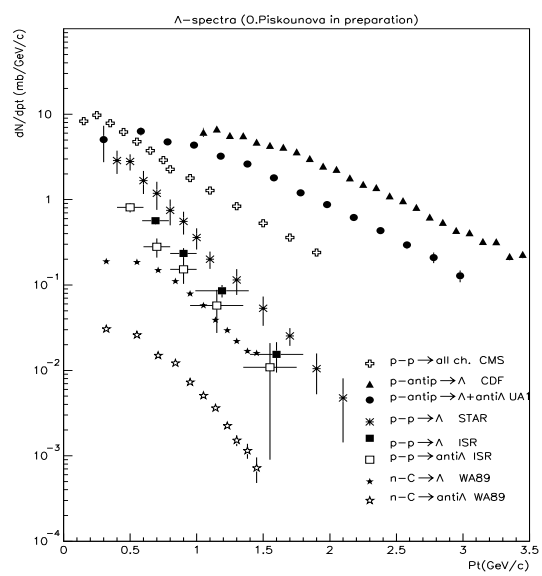


Figure 5: Strange baryon transverse momentum distributions from different experiments.

The available data of many high energy experiments on $p\bar{p}$ collisions [116, 117] as well as on $pp$ collisions of lower energies [118,119] and neutron-carbon reaction [120] are considered in this article in order to understand the influence of quark composition of beam particle on the shape of transverse momentum spectra of $\Lambda^0$ hyperon production as at high energy collider experiments as in low energy

fixed-target experiment (Fig. 5). The difference in $p_T$ spectra of $\Lambda^0$'s produced in high energy $pp$ and $p\bar{p}$ collisions can not be explained in the QCD theoretical models, because at the collider energies both interactions should give the multiple particle production due to Pomeron (or multi-Pomeron) exchange. The total cross section and the spectra in $pp$ and $p\bar{p}$ collisions are to be similar because of the Pomeron exchange between two interacting hadrons that should not be sensitive to the quark contents of colliding beams at high energies.

Unfortunately, this difference was not studied enough at ISR, where both projectiles were available. The important fact is that the latest collider experiments were carried out with antiproton beams. It was mistake to suggest that $pp$ and $p\bar{p}$ at high energy are giving the similar transverse momentum distributions. The spectra of hyperons that are produced with proton beam have a sharp exponential slope at low $p_T$, while the spectra with antiproton beam have not. The highest energy experiments (UA1 and Tevatron) shows harder $p_T$ spectra, that is not only the result of growing energy – it is the result of different form of transverse momentum distributions in different reactions.

From the point of view of the Quark-Gluon String Model (QGSM) [121], the most important contribution to particle production spectra in antiproton-proton reactions is due to antidiquark-diquark string fragmentation. Baryon hadroproduction spectra are sensitive to quark-diquark structure of interacting hadrons as well as to the energy splitting between these components. Asymmetric reactions may provide us with a new "stereoscopic" view on the hadroproduction mechanism. Measurements of $p_T$ spectra in antiproton-proton interactions at a variety of energies can thus constrain the contribution from the fragmentation of antidiquark-diquark string. This study may have impact not only on the interpretation of LHC results, but also on cosmic ray physics and astrophysics, where matter-antimatter asymmetry is being studied.

### DPMJET–III and $pp$ data from the LHC

*Johannes Ranft (Siegen University)*

Monte Carlo codes based on the two–component Dual Parton Model (soft hadronic chains and hard hadronic collisions) are available since 10–15 years: PHOJET for hadron-hadron (*h–h*) and photon-hadron ($\gamma$–*h*) collisions [122] and DPMJET-III based on PHOJET for hadron-nucleus (*h–A*) and nucleus-nucleus (*A–A*) collisions [123].

At the LHC particle production in $pp$ collisions was measured by the three Collaborations CMS, ALICE and ATLAS. Here we compare with measured pseudorapidity distributions at 900, 2360 and 7000 GeV c.m. energy, with $p_T$ distributions of charged hadrons at the same energies and with $\bar{p}$ to $p$ ratios. The problem to be solved at the beginning was, that DPMJET-III and all other event generators did predict pseudorapidity distributions rising slower with energy than the LHC data. To solve this problem we had to redetermine the parameters of DPMJET-III in such a way, that agreement with the data is achieved. We can present at the moment only one preliminary solution. In this solution we introduce an energy dependence in two of the DPMJET-III parameters. We call this a preliminary solution, since we think that also the new parameters should not depend on the energy. We are confident, that we will find soon such a solution, but at the moment all solutions with energy independent parameters have still problems.

We were able to present at the meeting charged pseudorapidity distributions which agree perfectly with the CMS data. We found also central antiproton to proton ratios in agreement with the ALICE data. The $p_T$ distributions of DPMJET-III agree with the CMS distributions. But one weakness of the $p_T$ comparisons is, that at present the average $p_T$ values at energies lower than the LHC energies are slightly higher than the data, this is also one problem which has to be solved. Finally, we find perfect agreement of charged hadron multiplicity distributions comparing DPMJET-III with the ALICE data.

# 3 Cosmic-rays at Ultra-High Energies: Experiments

### Results from the Pierre Auger Observatory

*Lorenzo Cazon*[17] *(LIP, Lisbon)*

The Pierre Auger Observatory is the largest cosmic ray (CR) observatory on Earth, covering 3000 km$^2$ of the high plateau in the Argentinian region of Pampa Amarilla [124]. It detects CR air showers in two complementary ways: an array of water-Čerenkov tanks samples the secondary particles at ground and fluorescence telescopes observe the longitudinal development of the electromagnetic cascade [125].

An energy spectrum has been recently published [126] covering the energy range from $10^{18}$ eV to above $10^{20}$ eV. The dominant systematic uncertainty stems from the overall energy scale, and is estimated to be 22%. The position of the ankle at $\log_{10}(E_{ankle}/eV) = 18.61 \pm 0.01$ and a flux suppression above $\log_{10}(E_{1/2}/eV) = 19.61 \pm 0.03$ have been determined. The suppression is similar to what is expected from the GZK effect for protons or nuclei as heavy as iron, but could also be related to a change of the injection spectrum at the sources.

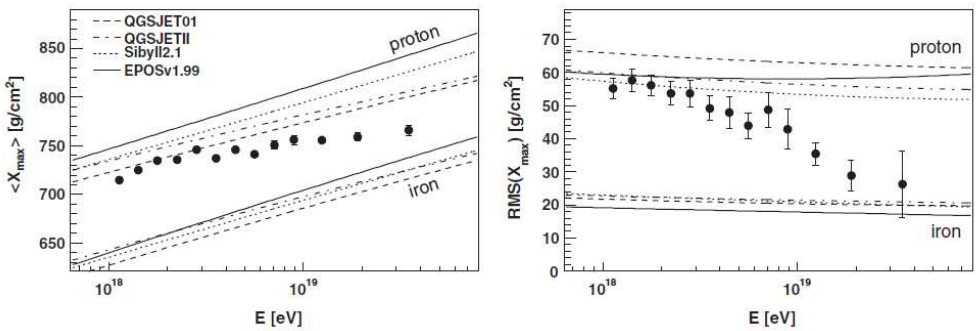


Figure 6: $\langle X_{max} \rangle$ and RMS($X_{max}$) measured by Auger compared to different hadronic interaction models.

Analyses of both the mean values and the fluctuations of the shower maximum $\langle X_{max} \rangle$ (plotted in Fig. 6, in comparison with the prediction of different hadronic interaction models) reveal a change in the energy dependence of the composition around the ankle and a gradual increase of the average mass of cosmic rays with energy, provided that there are not significant changes in the properties of the hadronic interactions at ultrahigh energies. More details can be found in [127].

A detailed comparison of the muonic and electromagnetic content of the air showers far from the core shows an excess in the number of muons of $\sim 50\%$ compared to protons simulated with QGSJET-II ($\sim 30\%$ excess compared to iron) [128]. This analysis also suggests a larger energy scale (27%) with respect to the fluorescence detector, being still compatible within the systematic uncertainties.

Showers initiated by photons and neutrinos have distinct signatures compared to showers initiated by protons or other nuclei, being possible to discriminate them [129, 130] and set bounds on their fluxes. The neutrino and photon bounds already exclude 'top-down' models for the production of ultra-high energy cosmic rays, favoring acceleration in astrophysical scenarios.

In 2007, it was shown that the arrival directions of CRs with energy in excess of 55 EeV correlated with the positions of nearby AGN [131]. As further data has been added, the degree of corre-

[17]On behalf of the PAO Collaboration. Support FCT-Portugal (CERN/FP/109286/2009) and ECT* are acknowledged.

lation has decreased from $69^{+11}_{-13}$% to $38^{+7}_{-6}$%, to be compared with the 21% expected if the flux were isotropic [132]. The region of the sky with the largest observed excess with respect to isotropy corresponds to Cen A, which is the closest AGN. Nevertheless, at present there are multiple astrophysical models of anisotropy which are fully consistent with the observed distribution of arrival directions. While a correlation of arrival directions with nearby matter on small angular scales is plausible for protons above 55 EeV, it is puzzling if the CRs are heavy nuclei as suggested by the $X_{max}$ measurements, since they are expected to undergo large deflections due to the galactic and extragalactic magnetic fields. Definitive conclusions must await additional data.

**HiRes results: The final word (almost)**

*Douglas R. Bergman*[18] *(Univ. of Utah)*

The High Resolution Fly's Eye (HiRes) experiment was a ultra-high energy cosmic ray detector operating in Utah from 1997-2006. It used the fluorescence technique to detect cosmic ray air showers in stereo using two detector sites.

HiRes was the first experiment to observe the GZK cutoff. We observed the break with a significance of greater than 5σ in monocular mode [2] and confirmed that discovery in stereo mode [133]. The position of the break is consistent with what is expected for extragalactic protons as measured with Beresinki's $E_{1/2}$ test [134].

HiRes has made a direct measurement of cosmic ray composition at energies above $10^{18.2}$ eV using both the average $X_{\rm max}$ technique and by measuring the width of the $X_{\rm max}$ distribution [135]. Both show a composition consistent with pure protons. We note that great care must be taken to account for both trigger and reconstruction biases for the mean $X_{\rm max}$ measurement. We also note that the RMS is a biased estimator of the width of a non-Gaussian distribution; we use a Gaussian fit to the central part of the distribution (within twice the RMS of the mean) as a better estimator of the width. HiRes also measured the average width of individual showers. This also agrees with a protonic composition.

HiRes has made a number of searches for anisotropy in the arrival directions of cosmic rays. We observed none: no correlation with AGN's [136], no correlation with the local large scale structure as determined by galaxy surveys [137].

**Telescope-Array results**

*Nobuyuki Sakurai*[19] *(Osaka City Univ.)*

Telescope Array (TA) is a largest ultra high energy cosmic ray detector in northern hemisphere. Operation was started about 3 years ago, and the gathered data have delivered the interesting results on the extremely high energy cosmic rays. The detector consists of 507 plastic scintillation detectors (SD) which cover the ground area of 680 km$^2$ in 1.2 km mesh and 3 fluorescence telescope stations (FD) which surround the scintillator detector array and look inward. Each detector of SD has 2 layers of plastic scintillator plate of 3 m$^2$ area and 1.2 cm thickness. For FD, Telescope Array adopts two different types of telescopes. Two FD stations, which are called as BRM-FD and LR-FD, are newly developed for Telescope Array. One FD station which is called as MD-FD consists of the telescopes which had been operated as Hires-I detector.

[18]On behalf of the HiRes collaboration.
[19]On behalf of the Telescope-Array collaboration.

We analyze energy spectra of ultra high energy cosmic ray using 3 different data sets: FD-mono, Hybrid and SD. In the FD-mono analysis, MD-FD data is analyzed by the same program as HiRes-I. And we obtained energy spectrum which is consistent with HiRes result. This means that HiRes-I detectors which was moved to Telescope Array site have reproduced HiRes result. The Hybrid energy spectrum is obtained from the analysis which use both of FD data and SD data in order to improve the geometrical reconstruction, although its energy is reconstructed as same as FD analysis. The energy spectrum obtained by the hybrid analysis is consistent with FD-mono result. TA SD energy spectrum is also consistent with spectra from both of FD-mono analysis and the hybrid analysis. In analysis of SD data, SD energy scale is scaled so as to agree with FD energy scale using the result of hybrid analysis. Primary composition is studied using the shower maximum ($X_{max}$) observed by FD stereo data. In the energy region of $10^{18.6} \sim 10^{19.3}$ eV, the averaged $X_{max}$ is consistent with the proton primary hypothesis. Arrival direction study shows no correlation with Active Galactic Nuclei so far. The existence of ultra high energy photon is studied using the shower front curvature observed by SD, but no candidate is found in data. Electron LINAC (ELS) is installed in front of BRM-FD to calibrate using the electron beam in this year. The ELS calibration is expected to improve the systematic error of FD drastically.

**ARGO-YBJ results**

*Ivan De Mitri*[20] *(INFN, Lecce)*

Cosmic ray physics in the $10^{12} - 10^{15}$ eV primary energy range is among the main scientific goals of the ARGO-YBJ experiment [138, 139]. The detector, located at the Cosmic Ray Observatory of Yangbajing (Tibet, P.R. of China) at 4300 m a.s.l., is a full coverage Extensive Air Shower array consisting of a carpet of Resistive Plate Chambers of about $6000\,\mathrm{m}^2$. The apparatus layout, performance and location offer a unique possibility to make a deep study of several characteristics of the hadronic component of the cosmic ray flux in an energy window marked by the transition from direct to indirect measurements. In this short summary we will focus on hadronic interaction studies that are being performed within the experiment in the primary energy range going from 1 TeV to 1 PeV.

The proton-air cross section has been measured. The total proton-proton cross section has then been estimated at center of mass energies between 70 and 500 GeV, where no accelerator data are currently available. Other hadronic interaction studies can be performed by exploiting the detector capability to have very detailed information on the shower front space-time structure and the lateral distribution function by also using the analog readout of the RPC's. Because of lack of space, here we will report on the $p$-air and $pp$ cross section measurement only.

The measurement is based on the shower flux attenuation for different zenith angles, i.e. atmospheric depths [140]. The detector location (i.e. small atmospheric depth) and features (full coverage, angular resolution, fine granularity, etc.) ensure the capability of reconstructing showers in a very detailed way. These features have been used to fix the energy ranges and to constrain the shower ages. In particular, different hit (i.e. strip) multiplicity intervals have been used to select showers corresponding to different primary energies. At the same time the information on particle density, lateral profile and shower front extension have been used to select showers having their maximum development within a given distance/grammage $X_{dm}$ from the detection level. This made possible the unbiased observation of the expected exponential falling of shower intensities as a function of the atmospheric depth through the $\sec\theta$ distribution. After the event selection, the fit to this distribution with an exponential law gives the slope value $\alpha$, connected to the characteristic length $\Lambda$ through the

[20] On behalf of the ARGO-YBJ collaboration.

relation $\alpha = h_0/\Lambda$. That is:

$$I(\theta) = A(\theta)\, I(\theta = 0)\, e^{-\alpha(\sec\theta - 1)} \tag{2}$$

where $A(\theta)$ accounts for the geometrical acceptance of each angular bin. The parameter $\Lambda$ is connected to the proton interaction length by the relation $\Lambda = k\lambda_{int}$, where $k$ depends on hadronic interactions and on the shower development in the atmosphere and its fluctuations [141]. The actual value of $k$ must be evaluated by a full MC simulation and it depends also on the experimental approach, the primary energy range and on the detector response. The $p$-air *production* [142] cross section is then obtained from the relation: $\sigma_{p-air}\,(\mathrm{mb}) = 2.41 \times 10^4/\lambda_{int}\,(\mathrm{g/cm^2})$, while several theoretical approaches can be used to get the corresponding $pp$ total cross section $\sigma_{pp}$ [143].

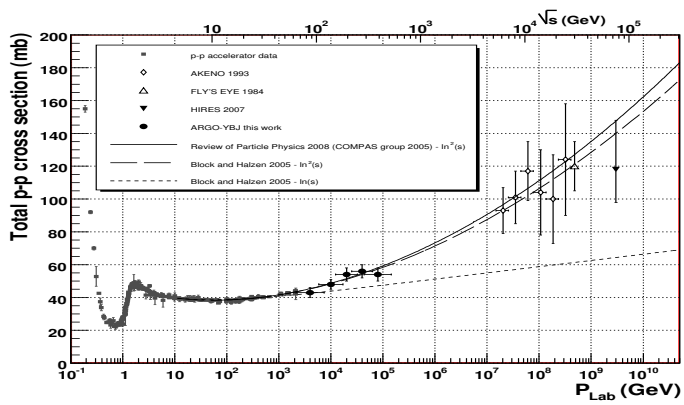


Figure 7: The $pp$ total cross section obtained by ARGO-YBJ, together with results published by other cosmic ray and accelerator experiments [140].

Results are shown in Fig. 7. As can be seen, ARGO-YBJ data lie in an energy region not yet reached by $pp$ colliders (and still unexplored by $p\bar{\mathrm{p}}$ experiments), favouring the asymptotic $ln^2(s)$ increase of total hadronic cross sections as obtained in [144] from a global analysis of accelerator data.

**KASCADE-Grande results**

*Paul Doll*[21] *(KIT, Karlsruhe)*

Testing of hadronic interaction models QGSJET-II-2 and EPOS 1.99 implemented in the CORSIKA program have been performed with KASCADE-Grande air shower data in the energy range of $10^{16}$ to $10^{18}$ eV [145, 146]. From the muon density investigations, the EPOS 1.99 model indicates that light abundances of primary cosmic ray particles would be needed to fit the data. On the other hand, the QGSJET-II-2 model describes the data with an intermediate primary abundance between proton and iron nuclei. The reconstructed all-particle energy spectra are presented by using the hadronic interaction models QGSJET-II-2 and EPOS 1.99. The resulting spectra show that the interpretation of the KASCADE-Grande data with EPOS 1.99 leads to significantly higher flux as compared to the QGSJET-II-2 result. More detailed investigations of EPOS 1.99 are still in work.

[21] On behalf of the KASCADE-Grande collaboration.

**IceCube results**

*Lisa Gerhardt*[22] *(LBL, Berkeley)*

High energy neutrinos offer a unique view of distant, energetic astrophysical objects, as they are neither bent by ambient magnetic fields nor absorbed by the interstellar medium. Possible sources of neutrinos include active galactic nuclei, gamma ray bursts, the highest energy cosmic rays, and interactions of exotic objects. The IceCube neutrino detector uses the ice at the South Pole as a Čerenkov medium for the detection of high energy neutrinos. It is composed of an in-ice, three-dimensional array of photomultiplier tubes [147] and a surface air shower array. Construction of the IceCube detector began in 2005 and was finished in 2010, bringing the detector to its full cubic kilometer size. Using data from the partially constructed detector, the IceCube Collaboration has searched for point sources of neutrinos [148, 149] and found results consistent with the expectation from the background of atmospheric neutrinos. It has set stringent upper limits on the diffuse fluxes of extremely high energy neutrinos [150] and on the flux of neutrinos in coincidence with Gamma-Ray Bursts [151] and has set limits on the accumulation of dark matter in the Sun [152, 153]. It has measured the flux of atmospheric neutrinos up to 400 TeV [154] and the anisotropy of the arrival directions of cosmic rays with a median energy of 20 TeV [155]. IceCube data collection continues.

[22] On behalf of the IceCube collaboration.

# 4 Cosmic-rays at Ultra-High Energies: Theory

### Open problems in cosmic ray physics and the importance of understanding hadronic interactions

*Ralph Engel (KIT, Karlsruhe)*

In Fig. 8, a compilation of measurements of the all-particle spectrum of cosmic rays is shown (from [156], updated). The most striking features are the knee at about $3 \times 10^{15}$ eV, the ankle between $10^{18} - 10^{19}$eV, and the suppression of the flux at the very highest energies. Understanding the origin of these characteristic breaks in the power-law of the flux is key to identifying the galactic and extragalactic sources of cosmic rays and the corresponding particle acceleration and propagation mechanisms.

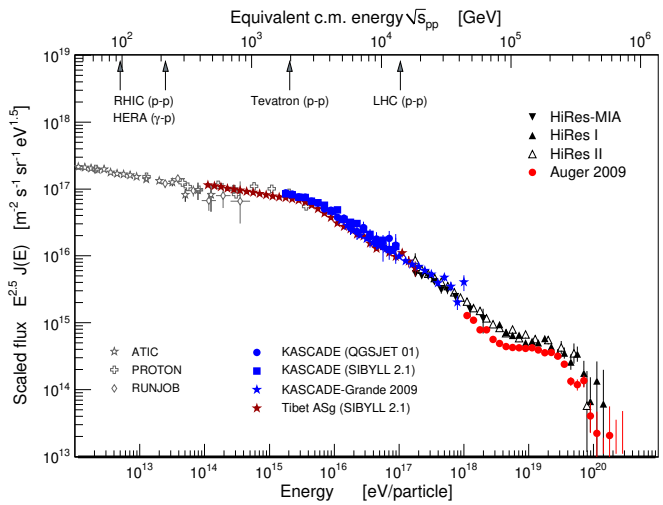


Figure 8: The all-particle flux of cosmic rays. For references to the data see [156].

For example, if the knee in the flux stems from features of diffusive shock acceleration processes it is expected that the fluxes of individual elements will exhibit knee-like features shifted in energy according to the magnetic rigidity $\sim E/Z$. Similarly, particle physics scenarios lead to the prediction of a scaling with mass number $\sim E/A$. Many other models have been developed for the knee, for example [157, 158] – for a review, see [159]. Similarly, there are several interpretations of the ankle. It seems natural to assign this feature to the transition between galactic and extragalactic cosmic ray sources [160]. Alternatively, in the dip model the ankle is the imprint of $e^+e^-$ pair production in extragalactic propagation [161], requiring a proton-dominated composition.

All these model scenarios differ in the predicted composition, making the accurate measurement of the mass composition and its evolution with energy a prerequisite to making progress in the field. Currently the largest uncertainty in the composition interpretation of air shower data is related to the description of hadronic interactions that has to be done with phenomenological models [162]. Measurement of multiparticle production at HERA, RHIC and LHC and using the data for refining existing interaction models will allow us to make significant progress in reducing this uncertainty.

**UHECRs and hadronic interactions**

*Paolo Lipari (Roma)*

The interpretation of the data on the Ultra High Energy Cosmic Rays requires an understanding of the development of hadronic showers and therefore a sufficiently accurate description of the properties of hadronic interactions. Since the energy spectrum of CR extends up to $E \sim 10^{20}$ eV, this requires an extrapolation to the c.m. energy of $\sqrt{s} \sim 430$ TeV.

The observations of fluorescence light, pioneered by the Fly's Eye collaboration, allows one to estimate the energy of a CR particle in a quasi–calorimetric way, with only little model dependence. The study of the shape of the longitudinal shower development allows one in principle to determine the mass number $A$ of the primary particle, but is also strongly dependent from the hadronic interaction properties. The position of the maximum of the shower longitudinal development $X_{\max}$ is a good indicator of $A$. The average $X_{\max}$ for a primary particle of energy $E$ and mass $A$, in reasonably good approximation, is given by:

$$\langle X_{\max}^{(A)}(E)\rangle \simeq \left\langle X_{\max}^{(p)}\left(\frac{E}{A}\right)\right\rangle \simeq X_0 + D_p\ \log\left(\frac{E}{A}\right) = X_0 + D_p\ \log E - D_p \log A \tag{3}$$

(the quantity $D_p$ is known as the "elongation rate"). This equation allows one to estimate the average mass (or $\langle \log A\rangle$) and the evolution with energy of the composition of UHECR, that is $d\langle \log A\rangle/dE$, if one has a good theoretical control of the model dependent quantities $X_0$ and $D_p$. It is therefore necessary to estimate the systematic uncertainty in the calculation of these quantities. It is also interesting to discuss what properties of the hadronic interactions determine $X_0$ and $D_p$. The main contributions come from the hadron interactions lengths (including the interaction lengths of mesons) and the inclusive energy spectrum of secondary particle in the projectile fragmentation region. The results that can be obtained at LHC with a precision measurement of the $pp$ cross section and of particle production properties will be important in constraining the models.

It is interesting to note that it is in principle possible to determine the composition of CR without any use of shower development, and therefore use the CR measurements to obtain information about the properties of hadronic interactions. One possibility is the observation of the imprints of energy losses on the observed energy spectrum (since the kinematical thresholds for the processes of $e^+e^-$ pairs and pion production are $A$ dependent), and the estimate of the deviation due to astronomical magnetic fields (that depends on $Z$). This could in principle allow one to determine properties of hadronic interactions from CR observations. The observations are at this point inconclusive. The energy scale of the HiRes detector is consistent with the hypothesis of attributing the "ankle" spectral feature, and the high energy suppression with energy loss imprints on a smooth spectrum strongly dominated by protons, but this interpretation is not consistent with the energy scale of the AUGER experiment. The AUGER collaboration has observed a correlation between the direction of the highest energy particles with potential extragalactic sources but the interpretation of the results remains ambiguous.

The study of the width of the distribution in the measurement of $X_{\max}$ also allows one to estimate the mass composition of CR, since the development of large $A$ primary particle has smaller fluctuations. The results of the AUGER experiment suggest that the highest energy particles are large $A$ nuclei, however these results are not confirmed by results of the HiRes and Telescope Array collaborations.

**On the relation between air shower predictions and features of hadronic interactions**

*Ralf Ulrich (KIT, Karlsruhe)*

The nature of cosmic ray particles at the very highest energies is still not understood. Even with experiments like the Pierre Auger Observatory [163], HiRes [164] and Telescope Array [165] delivering large quantities of high quality data, it is not straightforward to interpret these data. The fundamental problem is that the observations are very indirect: Only extensive air shower cascades, which are initiated by the cosmic ray primaries, are observed. For an accurate analysis of these air shower data a detailed understanding of interactions in the cascades is required. The particle production characteristics that are important in the context of air showers are interactions at energies of up to $\sqrt{s} \sim 350$ TeV and particle production in the very forward direction ($\eta > 6$). Particle production characteristics in this phase space have a strong impact on the modelling of the evolution of air shower cascades [166].

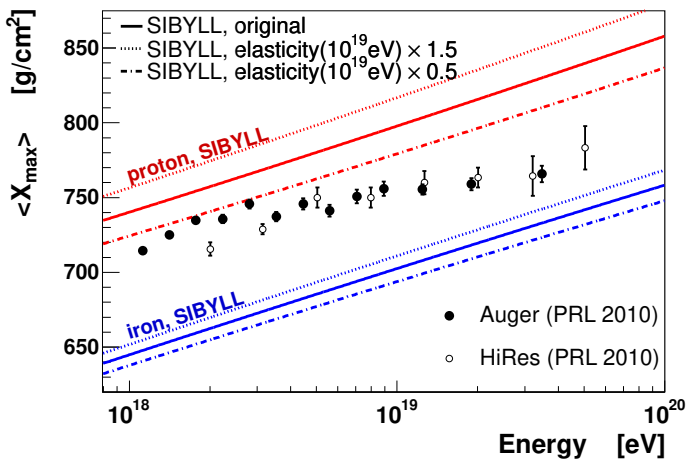


Figure 9: Measured average depth of the shower maximum [167,168] of UHE cosmic rays compared to SIBYLL predictions with a modified extrapolation of the elasticity to ultra-high energies.

In Figure 9 we demonstrate this at the example of the elasticity, $k_{\mathrm{ela}} = E_{\mathrm{max}}/E_{\mathrm{tot}}$, of interactions. It is shown that the interpretation of cosmic ray data relies on the detailed understanding of hadronic interaction physics. The LHC has the potential to significantly reduce the uncertainties because of two reasons: Firstly, it operates at energies that are already very relevant in terms of cosmic ray observations and, secondly, it has significant capabilities to study the forward phase space of multiparticle production that are relevant for the air shower modelling.

**The event generator SIBYLL 2.1**

*Ralph Engel*[23] *(KIT, Karlsruhe)*

SIBYLL is an event generator optimized for simulating high energy interactions needed for the description of extensive air showers and for the calculation of inclusive muon and neutrino fluxes. In comparison to other event generators, a rather basic and straightforward model for the description of multiparticle production is implemented. The initial version of the model [169] was upgraded in 2000

[23] In collaboration with Eun-Joo Ahn, Thomas K. Gaisser, Paolo Lipari, and Todor Stanev.

to include post-HERA parton density parametrizations and to introduce multiple soft interactions and a better treatment of diffraction dissociation [170].

Proton/pion/kaon-proton collisions are simulated in terms of multiple partonic soft and hard interactions, where each such partonic interaction leads to two QCD color strings, which subsequently fragment into hadrons. Diffraction dissociation is implemented as two-channel model of excited states for projectile and target particles, similar to the Good-Walker model [171] of diffraction dissociation. The minijet cross section is calculated within the QCD-improved parton model using the parton density parametrization of Glück, Reya and Vogt [172]. Saturation is accounted for by introducing an energy-dependent transverse momentum cutoff for distinguishing soft and hard interactions [173].

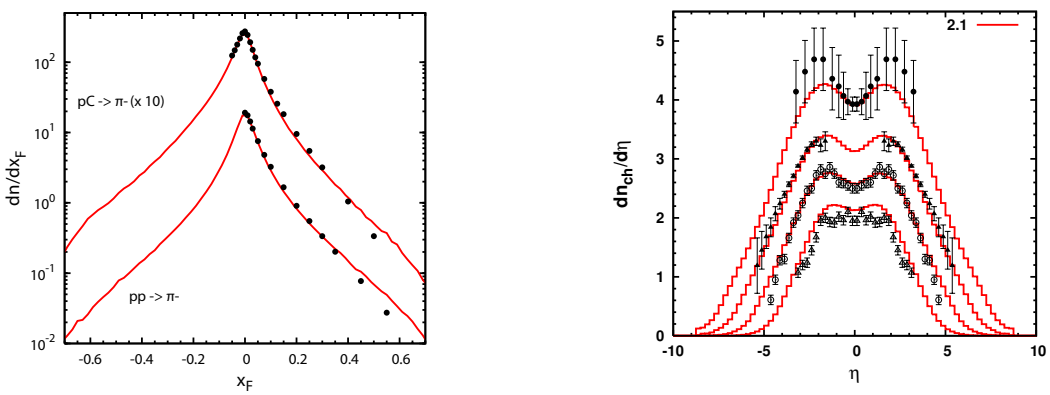


Figure 10: Comparison of SIBYLL predictions with fixed target data from NA49 [174] at $E_{\rm lab} = 158\,\text{GeV}$ (left) and different data sets from collider experiments (right) $\sqrt{s} = 54 - 1800\,\text{GeV}$ [170].

The scattering of hadrons off nuclei is modeled using the Glauber approximation. Realistic shell model distributions for the nucleon densities in the different nuclei are implemented [175]. The semi-superposition model is used for the description of the interaction of nuclei as beam particles with air [176]. The MC results are compared to fixed-target and collider data in Fig. 10.

**Pomeron calculus: cross sections, diffraction and MC simulation**

*Sergey Ostapchenko (NTNU, Trondheim)*

Monte Carlo (MC) generators of hadronic interactions are standard tools for data analysis in high energy collider and cosmic ray (CR) fields. A general framework for developing such generators is provided by the Reggeon Field Theory [177]. The key technique is the one proposed by Abramovsky, Gribov and Kancheli (AGK) [178], which allows one to relate partial cross sections for various configurations of hadronic final states to certain unitarity cuts of elastic scattering diagrams. The procedure generally requires the knowledge of the amplitude for an "elementary" elastic rescattering process ("Pomeron exchange") which corresponds to an underlying microscopic parton cascade, of the vertices for Pomeron-hadron coupling, and of the vertices for Pomeron-Pomeron ($I\!P I\!P$) interactions, if non-linear interaction effects are to be taken into account. In principle, all the three ingredients may be specified using different approaches, ranging from purely phenomenological parametrizations to BFKL-based treatment. In practice, one usually considers "soft" and "semihard" contributions to the elastic rescattering process, depending on whether it is dominated by a purely nonperturbative soft parton cascade or parton evolution extended to moderately large virtualities $|q^2|$. While soft parton evolution is described by phenomenological parametrizations (e.g., as soft Pomeron emission), its

extension to higher $|q^2|$ is typically treated within the DGLAP formalism.

It is worth stressing that the starting point for a development of a MC generator is the derivation of the complete set of partial cross sections for various hadronic final states. The latter are defined by the number of elementary particle production processes ("cut Pomerons") and by a particular arrangement of those cut Pomerons in rapidity-impact parameter space. Thus, calculations of partial cross sections involve full resummation of virtual (elastic) rescatterings which are described as uncut Pomeron exchanges. Such an analysis becomes especially simple when using eikonal vertices for Pomeron-hadron coupling and neglecting Pomeron-Pomeron interactions, which leads to the standard eikonal description of the elastic scattering amplitude and to simple expressions for partial cross sections. In particular, one arrives to the Poisson distribution for a number of elementary production processes for a given impact parameter.

However, the necessity to describe non-linear corrections to the interaction dynamics, related to parton shadowing and saturation, forces one to take Pomeron-Pomeron interactions into account, which significantly complicates the formalism. Indeed, with the energy increasing, so-called enhanced ($I\!P I\!P$ interaction) graphs of more and more complicated topologies start to contribute significantly to the scattering amplitude and to partial cross sections for particular hadronic final states. Thus, dealing with enhanced diagrams, all order resummation of the corresponding contributions is a must, both for elastic scattering diagrams and for the cut diagrams representing particular inelastic processes. Secondly, it is far non-trivial to split the complete set of cut enhanced diagrams into separate classes characterized by positively-defined contributions which could be interpreted probabilistically and employed in a MC simulation procedure. While the first problem has been addressed in [179–181], the MC implementation of the approach has been discussed in [182]. Let us briefly list the main results of the analysis of Refs. [179–182].

- Non-linear contributions to the interaction dynamics are not small corrections, but dominate the high-energy behavior of hadronic cross sections and particle production [179, 180, 182].

- Unlike inclusive particle (jet) cross sections, partial cross sections of hadronic final states which involve high transverse momentum jets can not be expressed via universal parton distribution functions (PDFs) measured in DIS experiments; rather they depend on "reaction-dependent PDFs" which involve parton rescattering on both the parent (e.g., projectile) hadron and the partner (here, target) hadron [180]. In other words, collinear QCD factorization is inapplicable to exclusive hadronic final states.

- An analysis of partial contributions of different classes of enhanced diagrams has shown that neither a resummation of contributions of "fan"-like graphs or of a more general class of "net"-like enhanced graphs nor of the ones of "Pomeron loop" diagrams alone is sufficient for a correct description of hadronic cross sections in the high-energy limit [181]. Instead, both classes of diagrams have to be taken into account.

- Calculations of diffractive cross sections require a proper resummation of absorptive corrections to the contribution of diffractively cut sub-graphs, which seriously reduce the probability for a rapidity gap survival, in addition to the usual (eikonal) rapidity gap suppression (RGS) factor [181]. In particular, restricting oneself with the simplest triple-Pomeron contribution to single high mass diffraction cross section, one arrives to a contradiction with $s$-channel unitarity, even if the eikonal RGS factor is included.

- The complete set of unitarity cuts of elastic scattering diagrams can be re-partitioned into a number of positively-defined contributions which define partial cross sections for certain

"macro-configurations" of the interaction ($s$-channel unitarity) [182]. For each of those macro-configurations, the pattern of secondary particle production can be reconstructed in an iterative fashion using a MC procedure.

One has to mention, however, that the approach of [179–182] has a serious drawback of neglecting energy-momentum correlations between multiple scattering processes at the amplitude level [183]. Additionally, the discussed treatment uses phenomenological parametrization for Pomeron-Pomeron interaction vertices and neglects hard (high $|q^2|$) $I\!P I\!P$ coupling. Hence, the scheme is unable to describe the dynamical evolution of the saturation scale in hadron-hadron scattering.

**Understanding the "ridge" in proton-proton scattering at 7 TeV**

*Klaus Werner*[24] *(Subatech, Nantes)*

The CMS collaboration published recently results [20] on two-particle correlations in $\Delta\eta$ and $\Delta\phi$, in $pp$ scattering at 7 TeV. Most remarkable is the discovery of a ridge-like structure around $\Delta\eta = 0$, extended over many units in $\Delta\eta$, referred to as "the ridge", in high multiplicity $pp$ events. A similar structure has been observed in heavy ion collisions at RHIC, and there is little doubt that the phenomenon is related to the hydrodynamical evolution of matter. This "fluid dynamical behavior" is actually considered to be the major discovery at RHIC.

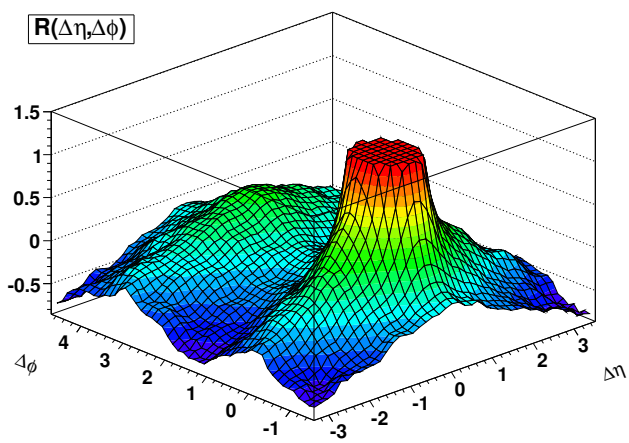


Figure 11: Two-particle correlation function $R$ versus $\Delta\eta$ and $\Delta\phi$ for high multiplicity events in $pp$ collisions at 7 TeV, as obtained from a hydrodynamical evolution based on flux tube initial conditions. We consider particles with $p_T$ between 1 and 3 GeV/c.

So does $pp$ scattering provide as well a liquid, just ten times smaller than a heavy ion collision? It seems so! We showed recently [184] that if we take exactly the same hydrodynamic approach which has been so successful for heavy ion collisions at RHIC [185], and apply it to $pp$ scattering, we obtain already very encouraging results compared to $pp$ data at 0.9 TeV. In this paper, we apply this fluid approach, always the same procedure, to understand the 7 TeV results. In Fig. 11, we show that our hydrodynamic picture indeed leads to a near-side ridge, around $\Delta\phi = 0$, extended over many units in $\Delta\eta$. For the pure basic string model, without hydro evolution, one finds no ridge! This shows that the hydrodynamical evolution "makes" the effect.

[24] In collaboration with Iu. Karpenko and T. Pierog.

It is easy to understand the origin of the ridge, in a hydrodynamical approach based on flux tube initial conditions, see [186]. Imagine many (say 20) flux tubes of small transverse size (radius $\approx 0.2$ fm), but very long (many units of space-time rapidity $\eta_s$ ). For a given event, their transverse positions are randomly distributed within the overlap area of the two protons. Even for zero impact parameter (which dominated for high multiplicity events), this randomness produces azimuthal asymmetries. The energy density obtained from the overlapping flux tubes shows an elliptical shape. And since the flux tubes are long, and only the transverse positions are random, we observe the same asymmetry at different longitudinal positions. So we observe a translational invariant azimuthal asymmetry!

If one takes this asymmetric but translational invariant energy density as initial condition for a hydrodynamical evolution, the translational invariance is conserved, and in particular translated into other quantities, like the flow. At a later time, at different space-time rapidities, the flow is more developed along the direction perpendicular to the principal axis of the initial energy density ellipse. This is a typical fluid dynamical phenomenon, referred to as elliptic flow. Important for this discussion: the asymmetry of the flow is again translational invariant, the same for different values of $\eta_s$. Finally, particles are produced from the flowing liquid, with a preference in the direction of large flow. This preferred direction is therefore the same at different values of $\eta_s$. And since $\eta_s$ and pseudorapidity $\eta$ are highly correlated, one observes a $\Delta\eta\Delta\phi$ correlation, around $\Delta\phi = 0$, extended over many units in $\Delta\eta$: a particle emitted a some pseudorapidity $\eta$ has a large chance to see a second particle at any pseudorapidity to be emitted in the same azimuthal direction.

### FLUKA **Monte Carlo**

*Maria Vittoria Garzelli*[25] *(INFN Milano & Univ. Granada)*

The FLUKA Monte Carlo code [187], also interfaced with the DPMJET code [188] for the treatment of nucleus-nucleus interactions, is being used in cosmic-ray physics. More detailed information on the physics models for *h-h*, *h-A*, $A-A$ interactions relevant for cosmic-ray Physics adopted in FLUKA and DPMJET is available in the literature [189]. Experimental observables involving muons, like cosmic $\mu^+/\mu^-$ charge ratios and the $\mu$ decoherence function of $\mu$ bundles detected underground, can be used to test the hadronic interaction models.

Cosmic $\mu^+/\mu^-$ charge ratios have been measured both by detectors at accelerator sites (L3+C, CMS, preliminary data from ALICE) and by passive underground experiments (Utah, MINOS, OPERA). The results of FLUKA simulations on $\mu^+/\mu^-$ charge ratio are shown together with available experimental data [190] in Fig. 12 (left). They turn out to be completely compatible with the CMS and L3+C data, whereas they slightly underestimate the MINOS data (however not completely confirmed by the OPERA ones, especially at the highest energies). A possible reason of this discrepancy is the fact that the $K^+/K^-$ charge ratio or the ratio between $K^+/K^-$ and $\pi^+/\pi^-$ charge ratios in FLUKA can be underestimated. The differences in the steepness of $x_{Feynman}$ distributions of $K^+$ and $K^-$ is also fundamental. To test these hypotheses new data on $K$ and $\pi$ production at high-energy accelerators are urgently needed.

The decoherence function, i.e. the distribution of the average distance between $\mu$ pairs in a bundle detected underground, is another observable that allows one to test the transverse structure predicted by the hadronic interaction models used to interpret the results of experiments on cosmic-rays. Such a measurement is highly sensitive to the $p_T$ distributions of $\pi$ and $K$ produced in the first stages of the shower formation process. We have verified that the decoherence function is robust against a change of the details of the cosmic-ray primary spectrum. FLUKA + DPMJET reproduces the experimental

[25] G. Battistoni, M.V. Garzelli, A. Margiotta, S. Muraro, M. Sioli for the FLUKA Collaboration

data from the MACRO experiment [191], as shown in Fig. 12 (right).

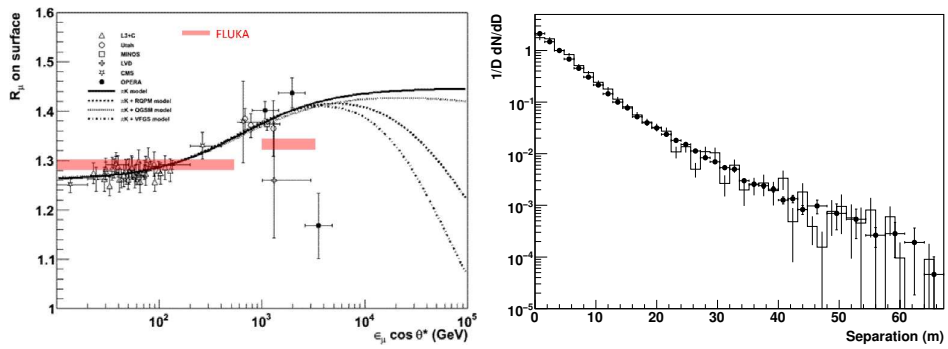


Figure 12: Left: $\mu^+/\mu^-$ charge ratio as a function of the surface energy $E_\mu cos\theta$: FLUKA simulation (pink bands representing an average charge ratio over all $E_\mu cos\theta$ values in the corresponding abscissa interval) vs. experimental data (Utah, LVD, L3+C, MINOS, CMS and OPERA). Right: decoherence distribution of $\mu$ pairs in a bundle (histogram: FLUKA+DPMJET; symbols: MACRO data)

### Comparison of model predictions to LHC data

*Tanguy Pierog (KIT, Karlsruhe)*

In April 2010, the ALICE [192] collaboration published for the first time the pseudorapidity distribution of charged particles at a center-of-mass energy of 7 TeV [26]. The analysis is based on a trigger called Inel>0 which consist of having at least one particle with $|\eta| < 1$. Unlike the Non Single Diffractive trigger, this does not include any model-based correction and allows then for an easy comparison with any hadronic interaction models. In Fig. 13 we compare the ALICE data at 900 GeV, 2.36 and 7 TeV with the models commonly used in air shower simulations, namely QGSJET 01 [193] and II-03 [194], SIBYLL 2.1 [170] and EPOS 1.99 [195], using the same trigger.

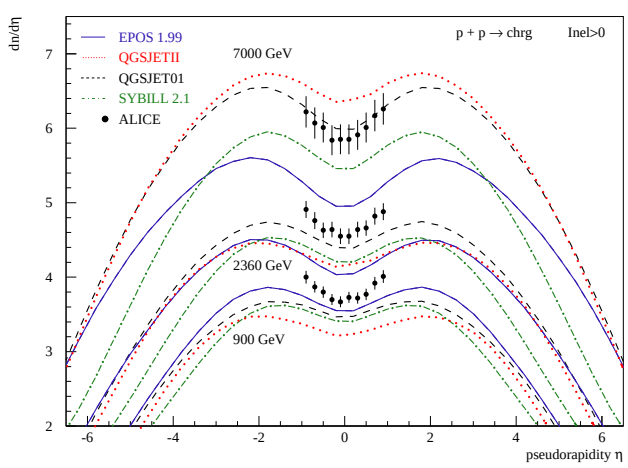


Figure 13: Pseudorapidity distribution of charged particles measured by ALICE in $pp$ ($Inel > 0$) collisions compared to the predictions of QGSJET 01 and II-03, SIBYLL 2.1, and EPOS 1.99 models.

Even if none of these MCs can reproduce perfectly all the data, it is interesting to notice that

the experimental results are well bracketed by the models used for cosmic ray analysis. The two extremes are EPOS 1.99 which underestimate the growth of the particle density and QGSJET II-03 which overestimates it. As a consequence we can say that the predictions of the Monte-Carlo models based on Regge field theory used for extended air shower analysis are compatible with the recent data from LHC, and hence do not show any tendency of dramatic change in minimum bias hadronic physics. Detailed results and dependence on trigger conditions not shown here indicate that soft physics is not yet completely understood.

# A List of participants

PARTICIPANTS:

Bruno Alessandro (*ALICE, Torino*),
Doug Bergman (*HiRes, Salt Lake City*),
Massimo Bongi (*LHCf, Florence*),
Armen Bunyatyan (*HERA, Yerevan & Hamburg*),
Lorenzo Cazon (*Auger, Lisbon*),
David d'Enterria (*Geneva*),
Ivan de Mitri (*ARGO-YBJ, Lecce*),
Paul Doll (*KASCADE-Grande, Karlsruhe*),
Ralph Engel (*Karlsruhe*),
Karsten Eggert (*TOTEM, Cleveland*),
Maria Garzelli (FLUKA, *Milano*),
Lisa Gerhardt (*IceCube, Berkeley*),
Stefan Gieseke (HERWIG, *Karlsruhe*),
Rohini Godbole (*Bangalore & Geneva*),
Jan Fiete Grosse-Oetringhaus (*ALICE, Geneva*),
Gösta Gustafson (*Lund*),
Thomas Hebbeker (*CMS, Aachen*),
Katsuaki Kasahara (*Tokyo*),
Yoshio Kitadono (*Tsukuba*),
Lev Kheyn (*CMS, Moscow*),
Joanna Kiryluk (*STAR, Berkeley*),
Paolo Lipari (*Roma*),
Sergey Ostapchenko (QGSJET, *Tromso*),
Tanguy Pierog (CORSIKA, *Karlsruhe*),
Olga Piskounova (QGSM, *Moscow*),
Johannes Ranft (DPMJET-*III, Siegen*),
Amir Rezaeian (*Valparaiso*),
Andrey Rostovtsev (*Moscow*),
Nobuyuki Sakurai (*TA, Osaka*),
Sebastian Sapeta (*Paris*),
Sebastian Schleich (*LHCb, Dortmund*),
Holger Schulz (*Berlin*),
Torbjörn Sjöstrand (PYTHIA *8, Lund*),
Lars Sonnenschein (*Tevatron, Aachen*),
Mark Sutton (*ATLAS, Sheffield*),
Ralf Ulrich (*Karlsruhe*),
Klaus Werner (EPOS *Nantes*),
Korinna Zapp (SHERPA, *Durham*)

# B Programme

**Monday, 29 November 2010**

| | |
|---|---|
| 09:00 *ECT* Director Welcome* (15') | A. Richter |
| 09:15 *Workshop introduction* (15') | D. d'Enterria |
| 09:30 *ATLAS QCD results* (30'+15') | M. Sutton |
| 10:15 *First CMS results* (30'+15') | T. Hebbeker |
| 11:00 *Particle multiplicity in p-p and HI collisions at colliders* (30'+15') | J.F. Grosse-Oetringhaus |
| 14:00 *LHCb QCD results* (30'+15') | S. Schleich |
| 14:45 *TOTEM results & perspectives* (30'+15') | K. Eggert |
| 15:30 *LHCf results* (30'+15') | M. Bongi |
| 16:00 *Tevatron QCD results* (30'+15') | L. Sonnenschein |
| 16:45 *HERA results of relevance for cosmic rays* (30'+15') | A. Bunyatyan |

**Tuesday 30 November 2010**

| | |
|---|---|
| 09:00 *Monte Carlo tuning at the LHC* (30'+15') | H. Schulz |
| 09:45 *Parton Correlations and fluctuations* (30'+15') | G. Gustafson |
| 10:30 SHERPA *Monte Carlo* (30'+15') | K. Zapp |
| 11:00 HERWIG *Monte Carlo* (30'+15') | S. Gieseke |
| 11:45 PYTHIA *8* (30'+15') | T. Sjöstrand |
| 14:00 *Total cross sections at very high energies* (30'+15') | R. Godbole |
| 14:45 *Jets and the Underlying Event* (30'+15') | S. Sapeta |

| | |
|---|---|
| 15:30 *Gluon Saturation at the LHC from CGC* (30'+15') | A. Rezaeian |

**Wednesday 1 December 2010**

| | |
|---|---|
| 09:00 *ALICE cosmic ray results* (30'+15') | B. Alessandro |
| 09:45 *CMS results of relevance for cosmic-rays* (30'+15') | L. Kheyn |
| 10:30 *STAR results of relevance for cosmic rays* (30'+15') | J. Kiryluk |
| 11:00 *Hadron production in collider experiments* (30'+15') | A. Rostovtsev |
| 11:45 *Baryon production at collider energies* (30'+15') | O. Piskounova |
| 14:00 DPMJET-*III: LHC predictions* (30'+15') | J. Ranft |
| 14:45 *Introduction to cosmic rays physis* (30'+15') | R. Engel |
| 15:30 *Cross section measurements using cosmic ray data* (30'+15') | R. Ulrich |

**Thursday 2 December 2010**

| | |
|---|---|
| 09:00 *IceCube results* (30'+15') | L. Gerhardt |
| 09:45 *Telescope-Array results* (30'+15') | N. Sakurai |
| 10:30 *Auger results* (30'+15') | L. Cazon |
| 11:00 *ARGO-YBJ results* (30'+15') | I. De Mitri |
| 11:45 *KASCADE-Grande results* (30'+15') | P. Doll |
| 14:00 *HiRes results* (30'+15') | D. Bergman |
| 14:45 *UHECRs and hadronic interactions* (30'+15') | P. Lipari |
| 15:30 *Air shower predictions and features of hadronic interactions* (30'+15') | R. Ulrich |

**Friday 3 December 2010**

| | |
|---|---|
| 09:00 SIBYLL *Monte Carlo* (30'+15') | R. Engel |
| 09:45 QGSJET-*II Monte Carlo* (30'+15') | S. Ostapchenko |
| 10:30 EPOS *Monte Carlo* (30'+15') | K. Werner |
| 11:00 FLUKA *Monte Carlo* (30'+15') | M. V. Garzelli |
| 11:45 *Comparison of UHCR models to LHC data* (30'+15') | T. Pierog |

## References


[1] K. Greisen, Phys. Rev. Lett. 16 (1966) 748–750; G. T. Zatsepin and V. A. Kuzmin, J. Exp. Theor. Phys. Lett. 4 (1966) 78.

[2] R. U. Abbasi *et al.* [HiRes Collab.], Phys. Rev. Lett. 100, 101101 (2008)

[3] J. Abraham *et al.* [Pierre Auger Collab.], Phys. Rev. Lett. **101** (2008) 061101

[4] D. d'Enterria, Proceeds. DIS'07, Munich; arXiv:0708.0551 [hep-ex].

[5] ATLAS Collab., Phys. Lett. B 688 (2010) 21-42; ATLAS-CONF-2010-024 (2010).

[6] ATLAS Collab., ATLAS-CONF-2010-046 (2010).

[7] ATLAS Collab., ATLAS-CONF-2010-029, ATLAS-CONF-2010-081 (2010).

[8] ATLAS Collab., accepted by EPJC, CERN-PH-EP-2010-034.

[9] ATLAS Collab., ATLAS-CONF-2010-083 (2010).

[10] ATLAS Collab., ATLAS-CONF-2010-077 (2010).

[11] ATLAS Collab., submitted to JHEP, CERN-PH-EP-2010-037 (2010).

[12] ATLAS Collab., ATLAS-CONF-2010-092 (2010).

[13] CMS Coll., JINST 3 (2008) S08004.

[14] CMS Collab., CMS PAS QCD-10-011 (2010).

[15] CMS Collab., Phys.Rev.Lett. 105 (2010) 211801.

[16] CMS Collab., arXiv:1011.5531 [hep-ex].

[17] CMS Collab., CMS PAS QCD-10-007 (2010).

[18] CMS Collab., CMS PAS QCD-10-014 (2010).

[19] CMS Collab., CMS PAS QCD-10-013 (2010).

[20] CMS Collab., J. High Energy Phys. 9 (2010) 91.

[21] CMS Collab., B. Wyslouch, "Pb Pb collisions in CMS", presentation CERN Dec 2, 2010.

[22] CMS Collab., CMS PAS EQK-10-002 (2010).

[23] CMS Collab., arXiv:1010.5994 [hep-ex].

[24] J.F. Grosse-Oetringhaus, K. Reygers, J. Phys. G **37** (2010) 083001

[25] ALICE Collab., Eur. Phys. J. C **68** (2010) 89

[26] ALICE Collab., Eur. Phys. J. C **68** (2010) 345

[27] V. Khachatryan *et al.* [CMS Collab.], Phys. Rev. Lett. **105** (2010) 022002

[28] A. Augusto Alves Jr *et al.* [LHCb Collab.], JINST 3, S08005 (2008).

[29] R. Aaij *et al.* [LHCb Collab.], Phys. Lett. B **693** (2010) 69.

[30] P. Z. Skands, Phys. Rev. D **82** (2010) 074018

[31] See TOTEM web-page: `http://totem.web.cern.ch/Totem/`

[32] E. Paré *et al.*, Phys. Lett. B, 242 (1990) 531–535

[33] O. Adriani *et al.*, CERN-LHCC-2006-004, LHCF-TDR-001 (2006)

[34] T. Sako *et al.*, Nucl. Instr. and Meth. A 578 (2007) 146–159

[35] R. D'Alessandro *et al.*, Acta Physica Polonica B 38 (2007) 829–838

[36] O. Adriani *et al.*, JINST 3 (2008) S08006

[37] M. Bongi *et al.*, Nucl. Instr. and Meth. A, 612 (2010) 451–454

[38] O. Adriani *et al.*, JINST 5 (2010) P01012

[39] H. Menjo *et al.*, Astroparticle Physics, In Press, 10.1016/j.astropartphys.2010.11.002

[40] DØ Collab., Nucl. Instrum. Methods Phys. Res., Sect. A **565**, 463 (2006).

[41] CDF Collab., Phys. Rev. D **71**, 032001 (2005) and refs. therein.

[42] DØ Collab., DØ-Note 6065-Conf (2010).

[43] CDF Collab., Phys. Rev. Lett. **102**, 222002 (2009).

[44] CDF Collab., accepted at Phys. Rev. D, arXiv:1007.5048 (2010).

[45] DØ Collab., DØ Note 6042-Conf FERMILAB-PUB-10-361-E (2010).

[46] CDF Collab., Phys. Rev. D **77**, 05204, hepex-0712.0604 (2008).

[47] CDF Collab., prelim. `http://www-cdf.fnal.gov/physics/new/qcd/ QCD.html` (2006).

[48] CDF Collab., Phys. Rev. Lett. **102**, 242001.

[49] CDF Collab., Phys. Rev. Lett. **99**, 242002 (2007).

[50] CDF Collab., Phys. Rev. Lett. **98**, 112001 (2007).

[51] DØ Collab., DØ-Note 6054-Conf (2010).

[52] CDF Collab., CDF/PUB/QCD/PUBLIC/10084 (2010).

[53] DØ Collab., Phys. Rev. D **81**, 052012 (2010).

[54] CDF Collab., Phys. Rev. D **82**, 034001, arXiv:1002.3146 (2010).

[55] CDF Collab., prelim. `http://www-cdf.fnal.gov/physics/new/qcd/ QCD.html` (2010).

[56] CDF Collab. Phys. Rev. Lett. **102**, 232002 (2009).

[57] STAR Collab., K.H. Ackermann *et al.*, Nucl. Instrum. Meth. **A499** (2003) 624.

[58] STAR Collab., B.I. Abelev *et al.*, Phys. Rev. Lett. **97** (2006) 252001; Phys. Rev. **D80** (2009) 111108; J. Adams *et al.*, Phys. Lett. **B616** (2005) 8; *ibid.* Phys. Lett. **B637** (2006) 161.

[59] STAR Collab., J. Adams *et al.*, Phys. Rev. Lett. **97** (2006) 152302.

[60] B. Surrow, to appear in the SPIN2010 conference proceedings.

[61] V.P. Goncalves and M.V.T. Machado, JHEP 0704 (2007) 028 and refs. therein

[62] STAR Collab., W. Xie *et al.*, POS DIS2010 (2010) 182; PHENIX Collab., A.Adare *et al.*, submitted to Phys. Rev. C; arXiv:1005.1627.

[63] M. Cacciari, P. Nason, and R. Vogt, Phys. Rev. Lett. **95** (2005) 122001.

[64] STAR Collab., B.I. Abelev *et al.*, Phys. Rev. **C80** (2009) 041902.

[65] G. C. Nayak *et al.*, Phys. Rev. **D68** (2003) 034003.

[66] STAR Collab., Z. Tang *et al.*, arXiv:1012.0233.

[67] STAR Collab., B.I. Abelev *et al.*, Phys.Rev. **D82** (2010) 12004.

[68] A.D. Frawley, T. Ullrich and R. Vogt, Phys. Rept. **462** (2008) 125.

[69] BRAHMS Collab., I. Arsene *et al.*, Phys. Rev. Lett. **93** (2004) 242303.

[70] STAR Collab., E. Braidot *et al.*, arXiv:1005.2378.

[71] D. Kharzeev, Y.V. Kovchegov, and K. Tuchin, Phys.Rev. **D68** (2003) 094013; J.L. Albacete and C.Marquet, Phys. Rev. Lett. **105** (2010) 162301 and refs. therein.

[72] STAR Collab., J. Adams *et al.*, Nucl. Phys. **A757** (2005) 102; PHENIX Collab., K. Adcox *et al.*, Nucl. Phys. **A757** (2005) 184; PHOBOS Collab., B. B. Back *et al.*, Nucl. Phys. A757 (2005) 28; BRAHMS Collab., I. Arsene *et al.*, Nucl. Phys. **A757** (2005) 1.

[73] STAR Collab., M.M. Aggarwal *et al.*, arXiv:1007.2613

[74] STAR Collab., B.I. Abelev *et al.*, Science **328** (2010) 58.

[75] E. Avsar, G. Gustafson, and L. Lönnblad, *JHEP* **07** (2005) 062, *ibid* **01** (2007) 012, *ibid JHEP* **12** (2007) 012.

[76] C. Flensburg, G. Gustafson, and L. Lönnblad, *Eur. Phys. J.* **C60** (2009) 233.

C. Flensburg and G. Gustafson, JHEP **1010** (2010) 014.

[77] M. G. Ryskin, A. D. Martin and V. A. Khoze, Eur. Phys. J. C **60** (2009) 249

[78] M. Bahr *et al.*, Eur. Phys. J. C **58** (2008) 639

[79] M. Bahr *et al.*, arXiv:0711.3137 [hep-ph].

[80] M. Bahr *et al.*, arXiv:0804.3053 [hep-ph].

[81] M. Bahr *et al.*, arXiv:0812.0529 [hep-ph].

[82] T. Sjöstrand and M. van Zijl, Phys. Rev. D **36** (1987) 2019.

[83] J. M. Butterworth, J. R. Forshaw and M. H. Seymour, Z. Phys. C **72** (1996) 637

[84] I. Borozan and M. H. Seymour, JHEP **0209**, 015 (2002)

[85] M. Bahr, S. Gieseke and M. H. Seymour, JHEP **0807** (2008) 076

[86] M. Bahr, S. Gieseke and M. H. Seymour, arXiv:0809.2669 [hep-ph].

[87] M. Bahr, J. M. Butterworth and M. H. Seymour, JHEP **0901** (2009) 065

[88] P. Bartalini *et al.*, arXiv:1003.4220 [hep-ex].

[89] M. Bahr, J. M. Butterworth, S. Gieseke and M. H. Seymour, arXiv:0905.4671 [hep-ph].

[90] C. Röhr, Diploma thesis, Karlsruhe Institute of Technology 2010

[91] A. A. Affolder *et al.* [CDF Collab.], Phys. Rev. D **65** (2002) 092002.

[92] D. E. Acosta *et al.* [CDF Collab.], Phys. Rev. D **70** (2004) 072002

[93] ATLAS-CONF-2010-031

[94] T. Sjöstrand, S. Mrenna and P. Skands, Comput. Phys. Comm. 178 (2008) 852

[95] T. Sjöstrand, S. Mrenna and P. Skands, JHEP05 (2006) 026

[96] R. Corke and T. Sjöstrand, Eur. Phys. J. C69 (2010) 1

[97] R. Corke and T. Sjöstrand, arXiv:1011.1759 [hep-ph]

[98] R. Corke and T. Sjöstrand, JHEP 01 (2010) 035

[99] R. M. Godbole, A. Grau, G. Pancheri and Y. N. Srivastava, Phys. Rev. D **72**, 076001 (2005).

[100] R. M. Godbole, A. Grau, G. Pancheri and Y. N. Srivastava, Eur. Phys. J. C **63**, 69 (2009)

[101] A. Corsetti, A. Grau, G. Pancheri,Y.N. Srivastava, Phys. Lett. **B 382**, 282 (1996)

[102] F. Cornet, C.A. Garcia Canal, A. Grau, G. Pancheri and G. Sciutto, Proceedings of the 31st ICRC, Lodz 2009.

[103] A. Grau, G. Pancheri,O. Shekhovtsova and Y. N. Srivastava, Phys. Lett. **B 693**, 456 (2009).

[104] M. Cacciari, G. P. Salam and S. Sapeta, JHEP **1004** (2010) 065

[105] D. Kar and R. Field (CDF Collab.), CDF/PUB/CDF/PUBLIC/9531, July (2008)

[106] M. Cacciari and G. P. Salam, Phys. Lett. B **659** (2008) 119

[107] M. Cacciari, G. P. Salam and G. Soyez, JHEP **0804** (2008) 005

[108] CMS Collab., CMS-PAS-QCD-10-005, July (2010)

[109] See e.g. F. Gelis *et al.*, arXiv:1002.0333; L. McLerran, arXiv:1011.3203, arXiv:1011.3204.

[110] E. Levin and A. H. Rezaeian, Phys. Rev. **D82** (2010) 014022; and arXiv:1011.3591.

[111] A. Dumitru *et al.*, arXiv:1009.5295.

[112] K. Aamodt *et al.* [ALICE Collab.], arXiv:1011.3916.

[113] Talk given by A. H. Rezaeian in this workshop.

[114] E. Levin and A. H. Rezaeian, Phys. Rev. **D82** (2010) 054003.

[115] A. Bylinkin, A. Rostovtsev, e-Print: arXiv:1008.0332 [hep-ph].

[116] UA1 Collab., G. Bocquet *et.al.*, Z. Phys. C **366** (1996) 441.

[117] CDF Collab., D. Acosta *et.al.*, Phys. Rev. D **72** (2005) 052001.

[118] STAR Collab., B.I. Abelev *et.al.*, Phys. Rev. C **75** (2007) 064901.

[119] ISR Collab., D.Drijard *et.al.*, Z.Phys. C **12** (1982) 217.

[120] WA89 Collab., M.I.Adamovich *et.al.*, Eur. Phys. J. C **26**(2003) 357.

[121] A.B. Kaidalov and K.A. Ter-Martirosyan, Sov. J. Nucl. Phys. **39**, 1545 (1984); **40**,211(1984); A.B. Kaidalov, Phys. Lett. B **116**, 459 (1982).

[122] R. Engel: Z. Phys. C **66**, 203 (1995), R. Engel and J. Ranft: Phys. Rev. D **54**, 4244 (1996)

[123] S. Roesler, R. Engel and J. Ranft: hep–ph/0012252, Proc. of Monte Carlo 2000, Lisboa, Oct.2000, Springer,p.1033

[124] Pierre Auger Collab., Nucl. Instruments and Methods A523 (2004), 50.

[125] Pierre Auger Collab., Nucl. Instruments and Methods in Phys. Research A613 (2010), 29-39; A620 (2010) 227; and arXiv:1010.6162

[126] Pierre Auger Collab., Phys. Lett. B685 (2010) 239.

[127] Pierre Auger Collab., Phys. Rev. Lett. 104 (2010) 091101.

[128] Pierre Auger Collab., Proceeds. 31st ICRC in Lodz, Poland (2009); arXiv:0906.2319.

[129] Pierre Auger Collab., Phys. Rev. D79 (2009), 102001.

[130] Pierre Auger Collab., Astropart. Phys. 31 (2009), 399.

[131] Pierre Auger Collab., Science 318 (2007), 939; Astropart. Phys. 29 (2008), 188.

[132] Pierre Auger Collab., Astropart. Phys. 34 (2010) 314.

[133] R. U. Abbasi *et al.* [HiRes Collab.], Astropart. Phys. 32, 53 (2009)

[134] V. S. Berezinsky and S. I. Grigor'eva, Ast. and Astrophys. 199, 1 (1988).

[135] R. U. Abbasi *et al.* [HiRes Collab.], Phys. Rev. Lett. 104, 161101 (2010)

[136] R. U. Abbasi *et al.* [HiRes Collab.], Astropart. Phys. 30, 175 (2008)

[137] R. U. Abbasi *et al.* [HiRes Collab.], arXiv:1002.1444.

[138] C. Bacci *et al.*, Astropart. Phys. **17** (2002) 151 and references therein

[139] I. De Mitri *et al.*, Nucl. Phys. **B** (Proc. Suppl.) **165** (2007) 66

[140] G.Aielli *et al.*, Phys. Rev. D **80** 092004 (2009) and references therein

[141] R.Ulrich *et al.*, New J. Phys. **11** (2009) 065018

[142] R. Engel *et al.*, Phys. Rev. D **58** (1988) 014019

[143] See e.g. T.K. Gaisser, Phys. Rev D **36** (1987) 1350 and M.M. Block, Phys. Rev D **76** (2007) 111503 and refs. therein

[144] M.M. Block and F.Halzen, Phys. Rev. **D72** (2005) 036006

[145] D. Kang *et al.*, arXiv:1009.4902 [astro-ph.HE].

[146] P. Doll *et al.*, arXiv:1010.2702 [astro-ph.HE].

[147] C. Wiebusch *et al.*, Nucl. Instr. Meth. Phys. Res. A **618** 139 (2010).

[148] R. Abbasi *et al.* [HiRes Collab.], Astrophys. Jour. Lett. **701** L47 (2009).

[149] R. Abbasi *et al.* [HiRes Collab.], Phys. Rev. Lett. **103**, 221102 (2009).

[150] R. Abbasi *et al.* [HiRes Collab.], Phys. Rev. D **82**, 072003 (2010).

[151] R. Abbasi *et al.* [HiRes Collab.], Astrophys. Jour. **710**, 346 (2010).

[152] R. Abbasi *et al.* [HiRes Collab.], Phys. Rev. Lett. **102**, 201302 (2010).

[153] R. Abbasi *et al.* [HiRes Collab.], Phys. Rev. D **81**, 057101 (2010).

[154] R. Abbasi *et al.* [HiRes Collab.], submitted to Phys. Rev. D (2010).

[155] R. Abbasi *et al.* [HiRes Collab.], Astrophys. Jour. **718** L194 (2010).

[156] J. Blümer, R. Engel, and J. R. Hörandel, Prog. Part. Nucl. Phys. 63 (2009) 293–338

[157] T. Stanev, P. L. Biermann, and T. K. Gaisser, Astron. & Astroph. 274 (1993) 902

[158] A. Erlykin, T. Wibig, and A. W. Wolfendale, arXiv:1009.0600

[159] J. R. Hörandel, Astropart. Phys. 19 (2003) 193–220

[160] A. M. Hillas, J. Phys. G31 (2005) R95–R131.

[161] V. Berezinsky, A. Z. Gazizov, and S. I. Grigorieva, Phys. Rev. D74 (2006) 043005

[162] J. Knapp, D. Heck, S. J. Sciutto, M. T. Dova, and M. Risse, Astropart. Phys. 19 (2003) 77–99

[163] J. Abraham *et al.* (Pierre Auger Collab.), Nucl. Instrum. Meth. A523 (2004) 50.

[164] R. Abbasi *et al.* (HiRes Collab.), Astrophys. J. 622 (2005) 910–926

[165] H. Kawai *et al.* (TA Collab.), Nucl. Phys. Proc. Suppl. 175-176 (2008) 221–226.

[166] R. Ulrich, R. Engel, and M. Unger, arXiv:1010.4310

[167] J. Abraham *et al.* (Pierre Auger Collab.), Phys. Rev. Lett. 104 (2010) 091101

[168] R. U. Abbasi *et al.* (HiRes Collab.), Phys. Rev. Lett. 104 (2010) 161101

[169] R. S. Fletcher, T. K. Gaisser, P. Lipari, and T. Stanev, Phys. Rev. D50 (1994) 5710–5731.

[170] E.-J. Ahn, R. Engel, T. K. Gaisser, P. Lipari, and T. Stanev, Phys. Rev. D 80 (2009) 094003

[171] M. L. Good and W. D. Walker, Phys. Rev. 120 (1960) 1857–1860.

[172] M. Glück, E. Reya, and A. Vogt, Z. Phys. C67 (1995) 433–448.

[173] L. V. Gribov, E. M. Levin, and M. G. Ryskin, Phys. Rept. 100 (1983) 1–150.

[174] C. Alt *et al.* (NA49 Collab.), Eur. Phys. J. C45 (2006) 343–381; *ibid* C49 (2007) 897–917

[175] R. J. Glauber and G. Matthiae, Nucl. Phys. B21 (1970) 135–157.

[176] J. Engel, T. K. Gaisser, T. Stanev, and P. Lipari, Phys. Rev. D46 (1992) 5013–5025.

[177] V. N. Gribov, Sov. Phys. JETP **26**, 414 (1968); *ibid.* **29**, 483 (1969).

[178] V. A. Abramovskii, V. N. Gribov and O. V. Kancheli, Sov. J. Nucl. Phys. **18**, 308 (1974).

[179] S. Ostapchenko, Phys. Lett. B **636**, 40 (2006); Phys. Rev. D **77**, 034009 (2008).

[180] S. Ostapchenko, Phys. Rev. D **74**, 014026 (2006).

[181] S. Ostapchenko, Phys. Rev. D **81**, 114028 (2010).

[182] S. Ostapchenko, Phys. Rev. D in press; arXiv:1010.1869.

[183] M. Hladik *et al.*, Phys. Rev. Lett. **86**, 3506 (2001).

[184] K. Werner, Iu. Karpenko, T. Pierog, M. Bleicher, K. Mikhailov, arXiv:1010.0400, submitted

[185] K. Werner, Iu. Karpenko, T. Pierog, M. Bleicher, K. Mikhailov, arXiv:1004.0805, to be published in Phys. Rev. C

[186] K. Werner, Iu. Karpenko, T. Pierog, arXiv:1011.0375

[187] A. Fassò *et al.*, CERN Yellow Report 2005-10, INFN/TC_05/11 (2005) 1; hep-ph/0306267. http://www.fluka.org

[188] S. Roesler *et al.*, hep-ph/0012252 and references therein. J. Ranft, Phys. Rev. D **51** (1995) 64.

[189] G. Battistoni *et al.*, Nucl. Phys. Proc. Suppl. **175-176** (2008) 88; 0711.2044; AIP Conf. Proc. **972** (2008) 449; arXiv:1002.4655.

[190] G.K. Ashley *et al.*, Phys. Rev. D **12** (1975) 20. L3 Collab., Phys. Lett. B **598** (2004) 15. MINOS Collab., Phys. Rev. D **76** (2007) 052003.CMS Collab., Phys. Lett. B **692** (2010) 83. OPERA Collab., EPJC **67** (2010) 25.

[191] MACRO Collab. hep-ex/9901027, Phys. Rev. D **60** (1999) 032001.

[192] K. Aamodt, *et al.*, [ALICE Collab.], JINST 3,S08002 (2008)

[193] N.N. Kalmykov, S.S. Ostapchenko and A.I. Pavlov, Nucl. Phys. Proc. Supl. 52B, 17 (1997).

[194] S. Ostapchenko, Phys. Rev. D **74**, 014026 (2006); AIP Conf. Proc. **928**, 118 (2007).

[195] K. Werner *et al.*, Phys Rev. C 74 044902 (2006).